ARL TECHNICAL REPORT 60-283

RESEARCH AND REPORTS ON AN OPTICAL AMPLIFIER

Joseph Lempert

Westinghouse Electric Corporation

MAY 1960

AERONAUTICAL RESEARCH LABORATORIES
AIR FORCE RESEARCH DIVISION

DISCLAIMER NOTICE

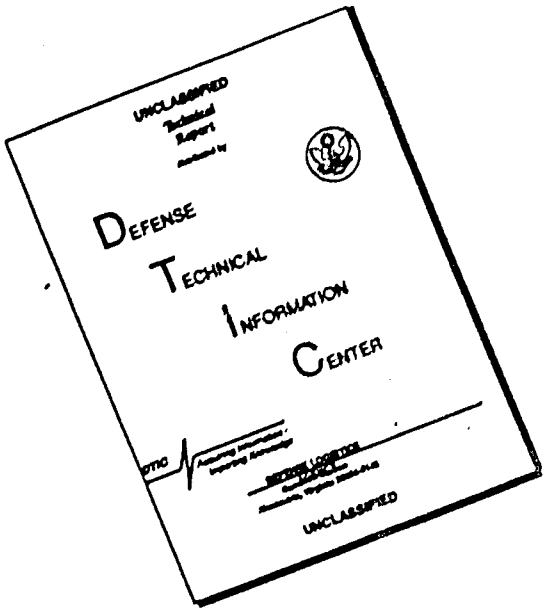

THIS DOCUMENT IS BEST QUALITY AVAILABLE. THE COPY FURNISHED TO DTIC CONTAINED A SIGNIFICANT NUMBER OF PAGES WHICH DO NOT REPRODUCE LEGIBLY.

ARL TECHNICAL REPORT 60-283

RESEARCH AND REPORTS ON AN OPTICAL AMPLIFIER

Joseph Lempert

Westinghouse Electric Corporation

MAY 1960

Contract No. AF 33(616)-2611
Project 7072
Task 70827

AERONAUTICAL RESEARCH LABORATORIES
AIR FORCE RESEARCH DIVISION
AIR RESEARCH AND DEVELOPMENT COMMAND
UNITED STATES AIR FORCE
WRIGHT-PATTERSON AIR FORCE BASE, OHIO

500 – July 1960 – 40-1148

FOREWORD

This technical report was prepared by Westinghouse Electric Corporation, Electronic Tube Division, Elmire, New York, on Task No. 70827, "Light Amplification", of Project 7072, "Research on the Quantum Nature of Light". The research reported here was initiated and administered by the Aeronautical Research Laboratory at Wright Air Development Center with Mr. Radames K. H. Gebel as Task Scientist.

This program was suggested by the Task Scientist on the basis of the following conclusions derived from research which he conducted within the Aeronautical Research Laboratory: (1) military needs can be met only by a closed circuit television type of light amplifier, in which preamilifier stages are used to provide an energy level sufficient to override fluctuations in the scanning beam of the transducer, and (2) it is theoretically possible for such a system to attain a useful sensitivity far greater than that of the unaided human eye, limited only by the ineluctable restrictions imposed by the statistical fluctuations in the rate of emission of photoelectrons and in the dark current of the first photocathode.

This report was not published at an earlier date because of its previous classification.

ABSTRACT

The purpose of this contract has been twofold. During Phase A, the object was to find through research new solutions which lead to new and improved types of pickup transducers which are potentially suitable for future development in the military field, especially under low light level conditions. Definite improvement has been accomplished in the threshold by extra dynode multiplication and by image preamplification. Phase B called for investigating the feasibility of producing an imaging pickup tube which would be capable of operating under the vibration encountered in an aircraft in flight. The feasibility of constructing image orthicons with considerably reduced microphonics, and suitable for use in aircraft, was established.

TABLE OF CONTENTS

TABLE OF CONTENTS (Cont.)

LIST OF GRAPHS

I. INTRODUCTION

Phase A - The work done under Phase A has indicated new solutions which may lead to new and improved types of pickup transducers potentially suitable for future development, especially under low light level conditions. The solutions conceived and the theoretical foundation laid during Phase A are being further investigated in our work under current contract AF33 (616) 3254 entitled, "Research on Optical Amplification". Details of theoretical results and experimental tests are given in the body of this report.

Briefly, they show that the quantum nature of light and of photoelectric emission will limit the ultimate sensitivity of a theoretically ideal imaging pickup tube in a manner which inter-relates scene brightness, scene contrast, speed of imaging, and obtainable resolution. For an ideal tube, making certain assumptions detailed below, this limits "seeing" a 500 TV line 100% contrast picture in the 1/30 second of a television frame to a scene brightness of about 4.2×10^{-6} ft. lamberts. Lower light levels are usable to produce an image in a longer time, an image with less resolution, or both. For example, with 1 second information storage time, a 20 TV line image should be "seen" at a scene brightness of about 1.2×10^{-8} ft. lamberts with a 20% scene contrast.

During work on this contract, the most sensitive camera tube in general use, the image orthicon, has been made to produce a 500 line image at a scene brightness, based on the above assumptions, of about 2.4×10^{-2} ft. lamberts. Using much longer information storage times and obtaining only sufficient resolution to resolve a gross image, the tube has been made to give a picture at a scene brightness of about 1×10^{-6} ft. lamberts. This data indicates that the best present image orthicons are still three or more orders of magnitude poorer than theoretically ideal imaging pickup tubes.

This experimental limit is shown to be set primarily by electrical fluctuations in the pickup tube and circuit which generate spurious signals that mask the information from lower light level scenes. Various approaches to better optical amplification considered during this research include special imaging optical preamplifier structures to increasing the light available to the pickup tube, various methods for increasing the optical amplification of the image orthicon type pickup tube, means for decreasing spurious signal generation in the tube, and consideration of other types of imaging pickup tubes, which may, when developed further, permit "seeing" with less light.

II. PHASE A - SENSITIVITY

Phase A was divided into three parts:

A. Theoretical study and evaluation of various approaches to the problems.
B. Experimentation to determine feasibility of items shown promising.
C. Experimental verification of the best combination of components and construction of models.

A. Theoretical Calculations

1. Basic Limitations Due to the Quantum Nature of Incident Light and the Photoelectric Emission Process

The illumination pattern on the photocathode of an imaging pickup tube consists of a flux of light photons or quanta. For presently known photocathodes, such as the Silver-Bismuth-Cesium Oxygen surface used in the image orthicon, one photoelectron is emitted for about every ten photons arriving at the cathode. On the average, the more photons arrive and more photoelectrons are emitted from a part of the photocathode which corresponds to a bright part of the scene being televised than from a dim part. However, both the arrival of photons and the emission of photoelectrons are random processes; and while the average number of photons arriving or electrons leaving a given part of the photocathode will for a stationary scene be a constant, if the average is taken over a sufficiently long time, the number arriving or leaving for any short time interval may be considerably different from the average. In particular, for a very dim scene, in which few light quanta arrive at the photocathode in a given time interval, say the 1/30 second of a commercial television scanning period, the number of photoelectrons leaving a bright part of the photocathode in a given frame time may actually be less than the number leaving a part of the cathode which corresponded to a dimmer part of the scene being viewed. Statistics tell us that for a random process, the root mean square deviation from the average value found in a given time interval is proportional to the square root of the average value of that time interval. That is, if N electrons leave on the average, the R.M.S. is $\sqrt{N}$. The relative size of the average photon flux or electron current to the deviation is therefore $\frac{N}{\sqrt{N}}$ or $\sqrt{N}$. This is a figure of merit, analogous to signal-to-noise ratio, and shows that the average signal will be stronger than the fluctuations by the factor $\sqrt{N}$.

For a picture element which receives 100 photons in a given information storage time, the signal-to-fluctuation ratio is $\sqrt{100}$ or 10. However, since there is, on the average, only one photoelectron emitted for every 10 photons, the number of electrons emitted in this time is only 10 and the signal-to-fluctuation ratio here is only $\sqrt{10}$ or 3.2. Thus, the effect of fluctuations in the photoelectron current is more serious and can be expected to the lower limit of the scene illumination from which a given quality image can be developed in a given time by even an ideal optical amplification device.

TABLE I

Resolution Which Can Be Perceived in Image as Function of Contrast and Number of Information Quanta in Signal

1	2	3	4	5	6	7
Per Cent Contrast	20 Line Resol. Flashes/Sec.	20 Line R Resol. Flashes/0.2 Sec.	100 Line Resol. Flashes/0.2 Sec.	200 Line Resol. Flashes/0.2 Sec.	400 Line Resol. Flashes/0.2 Sec.	500 Line Resol. Flashes/ 0.2 Sec.
100	900	180	4.5×10^3	1.80×10^4	7.2×10^4	1.1×10^5
70	2000	400	10^4	4×10^4	1.6×10^5	2.5×10^5
50	5000	1000	2.5×10^4	10^5	4×10^5	6.3×10^5
20	50000	10000	2.5×10^5	10^6	4×10^6	6.3×10^3
10	270000	54000	1.35×10^6	5.40×10^6	2.16×10^7	3.4×10^7

Note: This resolution is given in TV lines; i.e. total of blacks and whites. The original article measured resolution in line pairs.

Workers in the field have postulated that this threshold for "seeing" would be reached when the ratio of signal-to-fluctuation equalled one. Fortunately, a definitive investigation has been made of the limits on image formation set by this fluctuation or scintillation effect by Dr. John W. Coltman of the Westinghouse Research Laboratories* in connection with light amplification research for x-ray fluoroscopic purposes. The results of Dr. Coltman's work are given in Table #1 which shows that the number of information quanta (photoelectrons) required to build up an image in a given time in an ideal light amplifier increases with the number of resolution elements required for the image, and is far greater for low contrast images than for high. Unfortunately, most dimly lighted scenes of military interest are low in contrast. Column 1 gives the contrast in the image being viewed. . Column 2 gives the information quanta per second in Coltman's experiments. Coltman states that the information storage time of the eye is about 0.2 seconds, therefore columns 3 through 7 give the quanta in that information storage time necessary to build an image of the indicated quality. This same number of quanta must be present in the information storage time of an optical amplifier system to build a picture of that quality.

To apply this information to our work, we have prepared Table 2, which relates to highlight scene brightness (column 1),** and to photocathode illumination on the light amplifier (column 2). For this relation we assume the use of an f/0.85 lens with 75% optical tranmission such as the Zeiss-Jena R-Biotar or the Farrand Optical Co. Super Farron, and use the relation:

$$\text{Photocathode Illumination} = \frac{\text{Transmission}}{4f^2} \times \text{Scene Brightness}$$

For this lens:

Photocathode Illumination = 1/4 scene brightness

In column 3 giving the resultant photocurrent, we assume uniform illumination on a 0.96"x 1.28" area on a 60 microampere/lumen photocathode typical of the best in current widespread use. Columns 4, 5, and 6 show respectively the number of electrons leaving the photocathode in 1 second, in the 1/5 second storage time of the eye, and in 1/30 of a second. It is the local fluctuations in this photoelectron current which will set a lower limit to the scene illumination necessary for satisfactory image formation on a theoretically ideal light amplifier tube.

* Journal of the Optical Society of America, March, 1954, pages 234-237

** Scene illumination times reflectance of highlight objects.

TABLE II

Electrons Leaving Photocathode as Function of Light Level

1 Scene Brightness Foot Cantles	2 Illumination on Photocathodes in Foot Candles*	3 Amps Photo-** Current 1.6" Diagonal Rectangular Area	4 Electrons/sec. Photocathode (1 sec.storage)	5 Electrons/0.2 Sec. From Photocathode (0.2 Sec. Storage of Eye)	6 Electrons/ 1/30 Sec. from Photocathode (1/30 Sec. Storage)
10^{-10}	2.5×10^{-11}	1.28×10^{-17}	8×10^{1}	1.6×10^{1}	2.7×10^{0}
10^{-9}	2.5×10^{-10}	1.28×10^{-16}	8×10^{2}	1.6×10^{2}	2.7×10^{1}
10^{-8}	2.5×10^{-9}	1.28×10^{-15}	8×10^{3}	1.6×10^{3}	2.7×10^{2}
10^{-7}	2.5×10^{-8}	1.28×10^{-14}	8×10^{4}	1.6×10^{4}	2.7×10^{3}
10^{-6}	2.5×10^{-7}	1.28×10^{-13}	8×10^{5}	1.6×10^{5}	2.7×10^{4}
10^{-5}	2.5×10^{-6}	1.28×10^{-12}	8×10^{6}	1.6×10^{6}	2.7×10^{5}
10^{-4}	2.5×10^{-5}	1.28×10^{-11}	8×10^{7}	1.6×10^{7}	2.7×10^{6}
10^{-3}	2.5×10^{-4}	1.28×10^{-10}	8×10^{8}	1.6×10^{8}	2.7×10^{7}
10^{-2}	2.5×10^{-3}	1.28×10^{-9}	8×10^{9}	1.6×10^{9}	2.7×10^{8}
10^{-1}	2.5×10^{-2}	1.28×10^{-8}	8×10^{10}	1.6×10^{10}	2.7×10^{9}
1	2.5×10^{-1}	1.28×10^{-7}	8×10^{11}	1.6×10^{11}	2.7×10^{10}

* Assumed - an f0.85 lens having 0.75 light transmission.

** Assumed - 0.96 x 1.28" illuminated area on 60 microampere per lumen photocathode.

Note: Random quanta fluctuations are, by the nature of John W. Coltman's experiments, included in the data of this table.

Table 3 combines Tables 1 and 2 to predict, within the assumptions of an f/0.85 lens of 75% transmission illuminating a 0.96" x 1.28" area on a 60 microampere/lumen photocathode, the scene brightness required for an ideal optical amplifier to produce a usable image as a function of the contrast and resolution of the scene being viewed.

Three storage times are used, 1 second for tubes or systems which store the information (the image orthicon does this for low light levels), 1/5 second for non-storage light amplifiers viewed at low light levels by a human observer whose eyes will integrate for about this time, and 1/30 second, a standard TV frame time, for systems where the information is recorded or used in a computor frame by frame, or for viewing at high light levels.

Most of our work has been done with visual observation at light levels for which the visual storage time was probably intermediate between 1/30 and 1/5 second. At low light levels, the target of the present image orthicon tube stores energy over several frame times and partly evens out the effect of fluctuations in information quanta. Comparison of experimental results with Table 3 must therefore be made with qualifications.

Table 3 predicts that to obtain a 500 TV line image of a scene with 100% contrast in 1/30 second will require a scene brightness of about 4.2×10^{-6} f-c. For 70% contrast, perhaps more typical of the laboratory test patterns, the brightness doubles to 9.6×10^{-6} f-c. For 20% contrast, closer to values found for military objectives, the scene brightness for 500 line imaging in 1/30 second is about 2.4×10^{-4} f-c.

Lower light levels are usable to produce an image in a longer time, an image with less resolution, or both. For threshold imaging, that is, minimum scene brightness for reproduction of a gross image, we assume 20 lines resolution 20% contrast and a 1 second storage time. This gives a threshold scene brightness of about 1.2×10^{-8} f-c.

Within the assumptions made, the foregoing calculations are valid for any light amplifier and set limits for an ideal tube beyond which we cannot go. However, the assumptions may be modified, and recent information indicates that improved photocathodes have now been produced in the laboratory which have 3.5 times the efficiencies assumed here. Research toward photocathode improvement, larger lenses and photocathodes with electron optical minification, faster lenses, and longer information storage times, perhaps with several light amplifiers used in rotation to permit following the motion in the scene bring viewed, offer hope of lowering the theoretical light requirements for imaging a given scene with a given quality. Part of the research under this

TABLE III

SCENE BRIGHTNESS - FOOT LAMBERTS - REQUIRED FOR GIVEN RESOLUTION IN TV LINES
AS SET BY QUANTUM LIMITATIONS ONLY

Scene Contrast	TV Lines Resol.	Storage Time - 1 second				Storage Time - 1/5 second			
		20	200	400	500	20	200	400	500
100%		2.2×10^{-10}	2.2×10^{-8}	9×10^{-8}	1.4×10^{-7}	1.1×10^{-9}	1.1×10^{-7}	4.5×10^{-7}	7×10^{-6}
70%		5×10^{-10}	5×10^{-8}	2×10^{-7}	2×10^{-7}	3.2×10^{-9}	6×10^{-7}	1×10^{-6}	1.6×10^{-6}
50%		1.2×10^{-9}	1.2×10^{-7}	5×10^{-7}	8×10^{-7}	6×10^{-9}	6×10^{-7}	2.5×10^{-6}	4×10^{-6}
20%		1.2×10^{-8}	1.2×10^{-6}	5×10^{-6}	8×10^{-6}	6×10^{-8}	6×10^{-6}	2.5×10^{-5}	4×10^{-5}
10%		7×10^{-8}	7×10^{-6}	2.7×10^{-5}	4.4×10^{-5}	3.5×10^{-7}	3.5×10^{-5}	1.3×10^{-4}	2.2×10^{-4}

	Storage Time - 1/30 second			
100%	6.6×10^{-9}	6.6×10^{-7}	2.7×10^{-6}	4.2×10^{-6}
70%	1.5×10^{-8}	1.5×10^{-6}	6×10^{-6}	9.6×10^{-6}
50%	3.6×10^{-8}	3.6×10^{-6}	1.5×10^{-5}	2.4×10^{-5}
20%	3.6×10^{-7}	3.6×10^{-5}	1.5×10^{-4}	2.4×10^{-4}
10%	2.1×10^{-6}	2.1×10^{-4}	8.1×10^{-4}	1.3×10^{-3}

Assumptions included: Use of an ideal imaging tube with perfect storage and utilization of available quanta.

Note: This table was prepared by combination of Tables I and II and necessarily includes the same assumptions as these tables.

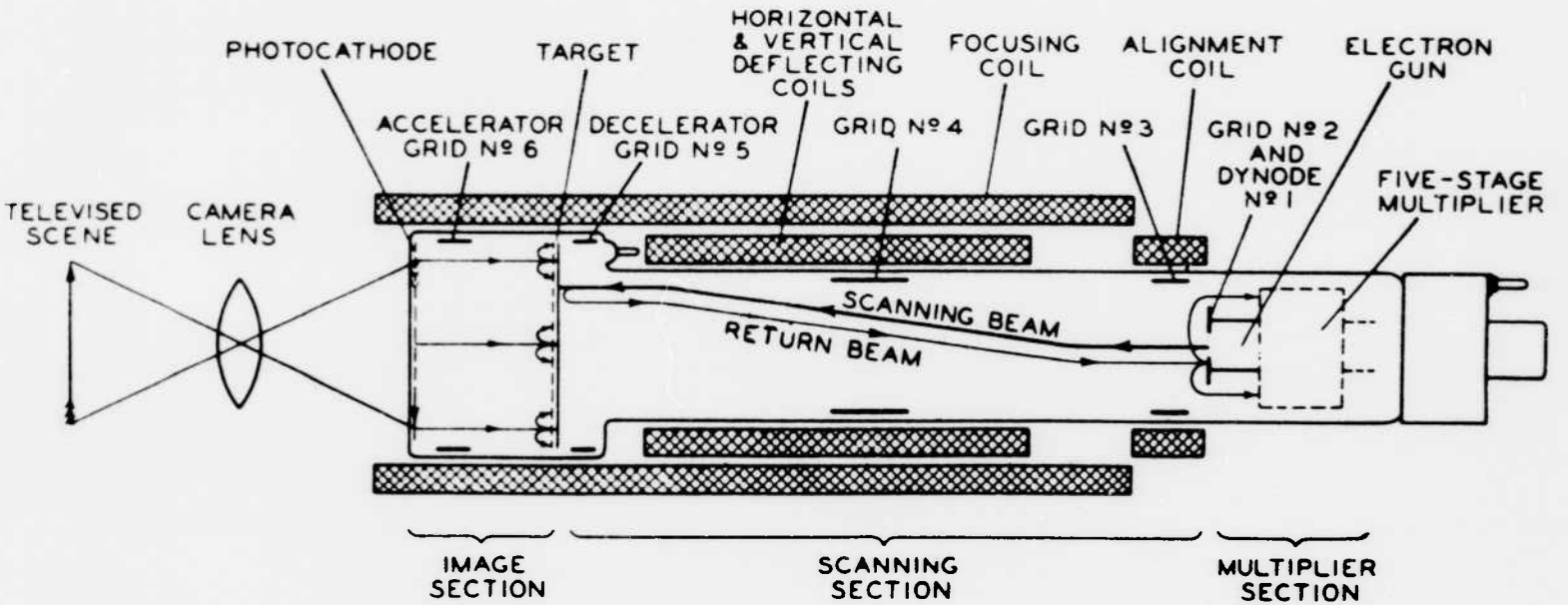

Figure 1. Schematic Arrangement, Image Orthicon Tube and Coils

contract has been on approaches which would lower this theoretical limitation.

In practice, as discussed below, the best imaging optical amplifiers are still two or more orders of magnitude worse than the calculated ideal tube and it is largely with attempts to close this gap that the research under this contract is concerned.

2. Limitations in the Standard Image Orthicon Due to Fluctuations In the Scanning Beam. (Figure 1)

The image orthicon, the most sensitive camera tube in general use, has been the starting point for work on this contract. In the image orthicon*, a photoelectric current density pattern corresponding to the image on the photocathode is directed at and focussed on a thin glass membrane or target with such energy that the secondary emission ratio of the target is greater than one. Therefore, in areas corresponding to illuminated areas in the image, the target accumulates a positive charge pattern. This charge pattern is "read" and neutralized by a low velocity electron beam which scans the other side of the target in the desired television or other scanning pattern. The scanning beam is composed of electrons, emitted in a random manner from the space charge at the cathode, which represent a constant current flow when averaged over a sufficiently long time. In any short time interval, however, the number of beam electrons passing a given point may vary widely.

In the image orthicon, this beam fluctuation current is almost completely added to the signal current representing the desired image, and forms a spurious signal which may completely mask the signal from a low light level scene. Because with the image orthicon it is thought to be a serious obstacle to approaching the theoretical light amplifier performance given above, much effort has been devoted to minimizing the effect of scanning beam fluctuations. Any means which will increase the amplitude of the signal current to be read off the target for a given scene brightness will increase the signal-to-fluctuations ratio, These means include more efficient photocathodes, larger photocathodes with appropriate lenses, light amplification, electron multiplication between the photocathode and the target, means for increasing the secondary emission ratio of the target, targets with different operating principles to obtain high current amplification in the target, and use of a long storage time between scans to accumulate a lot of signal for a given amount of beam fluctuation current. All of these approaches have been considered under this contract.

* For a complete description of image orthicon operation, see The Image Orthicon, A Sensitive Television Pickup Tube, A. Rose and P.K. Weimer and H.B. Law, Proc. I.R.E. (July 1946)

The effect of scanning beam fluctuations on low light level "seeing" may be calculated as follows:

For an emission limited diode, the RMS fluctuation current in amperes is

$$I_F = 5.66 \times 10^{-10} \sqrt{I_O B}$$

Where I_O = average anode current in amperes,
B = bandwidth in cycles per second of the following amplifier system.

For a space charge limited diode, the RMS fluctuation current is reduced by a smoothing action in the space charge. The electron gun in an image orthicon is not a diode. It is operated space charge limited, and although the above fluctuation formula has been used to give the fluctuations in an electron beam, the actual fluctuation current may be up to three times smaller.

The fluctuation energy is distributed uniformly throughout an extremely wide spectrum. The amount appearing in the output signal is therefore proportional to the bandwidth of the video amplifier and indicator system used to present the picture. As indicated above, the fluctuations in the picture information limit the resolution obtainable for very low light levels. To minimize the effects of scanning beam fluctuations, the bandwidth of the information handling system should be reduced to make the most of low light level signals. To do this properly, both vertical and horizontal resolution should be reduced together. This is, however, impractical in most TV camera equipment and was not attempted here.

On the contrary, most tests of experimental tubes were made with video amplifier pass bands from 8 to 20 megacycles using a standard 525 line TV raster.

To determine how seriously beam noise contributes to minimum light level limitation, we take some typical figures:

An image orthicon type tube has been made to reproduce a 500 line 80 % contrast picture at a scene brightness of about 6×10^{-3} foot lamberts, corresponding to 1.5×10^{-3} foot candles on the photocathode and therefore to 7.5×10^{-10} amperes of photocathode current in the white parts of the pattern. A typical image orthicon target has a secondary emission gain of 3 to 5. Electrons landing from the scanning beam must therefore neutralize a current of (using the lower figure,) $3 \times 7.5 \times 10^{-10} = 2.25 \times 10^{-9}$ amperes. It is estimated that about 10% of the beam electrons actually land on the target, therefore, the average beam current must be 10 times this large or 2.25×10^{-8} amperes. For a beam current of 2.25×10^{-8} amperes and an 8 megacycle bandwidth, the

RMS fluctuation current, from the temperature limited diode formula, is

$$I_F = 5.66 \times 10^{-10} \sqrt{2.25 \times 10^{-8} \times 8 \times 10^{6}}$$

$$= 23 \times 10^{-11} \text{ amps}$$

$$= 2.3 \times 10^{-10} \text{ amps}$$

The signal-to-fluctuations ratio is therefore

$$\frac{2.25 \times 10^{-10}}{2.3 \times 10^{-10}} \sim 10{:}1$$

The assumed beam fluctuations are not limiting sensitivity.

For a threshold picture, on a gross image, an image orthicon type tube was made to operate with about 1×10^{-6} foot lamberts scene brightness, corresponding to 2.5×10^{-7} f-c on the photocathode. A number of tubes were made to produce threshold images between this value and 8×10^{-6} foot lamberts, corresponding to 2×10^{-6} foot candles photocathode illumination. Using the above assumptions, this corresponds to a photocathode current of 5×10^{-13} amps, a signal current at the target of 1.5×10^{-12} amps, and a beam current of at least 1.5×10^{-11} amps.

The fluctuation current will be

$$I_F = 5.66 \times 10^{-10} \sqrt{1.5 \times 10^{-11} \times 8 \times 10^{6}}$$

$$= 5.66 \times 10^{-10} \sqrt{\frac{12 \times 10^{-5}}{1.2 \times 10^{-4}}}$$

$$= 6.2 \times 10^{-12} \text{ amps}$$

The ratio of target signal current to fluctuation current is therefore approximately $\frac{1.5 \times 10^{-12}}{6.2 \times 10^{-13}} = 0.24$

Thus, the beam fluctuation current may be a dominant limiting factor on optical amplification of lower light level scenes with an image orthicon. However, assumptions were made in this analysis which may make this calculated result too pessimistic. Target gains of much more than 3 have been measured for low light level imaging. Beam fluctuations may be as little as 1/3 the calculated value. Beam modulation percentage (percentage reading the target) may be higher than 10%.

Attempts to improve threshold by limiting the bandpass of the video amplifier have so far been unsuccessful. Further, fluctuations observed in threshold scenes appear to be predominantly in the lower frequencies, in the order of a few hundred kilocycles or a megacycle. This may indicate that other spurious signal sources are also acting to limit lower light level "seeing".

3. Camera Tube Signal Amplification Requirements

It is known that the equivalent fluctuation current generated in a "low noise" video amplifier input stage is about 2×10^{-9} amperes at the input.

To prevent degradation of the signal, the signal-to-fluctuations current here should be at least 5:1 .

Table 4 gives the amplification required in the pickup tube to provide an output signal of 1×10^{-8} amperes as a function of scene brightness.

Scene Brightness Ft. Lamberts	Photocathode* Current Amperes	Overall Gain Required in Tube For Signal-to- Fluctuations Ratio of** 1:1	5:1
10^{-10}	1.28×10^{-17}	1.6×10^{8}	8×10^{8}
10^{-9}	1.28×10^{-16}	1.6×10^{7}	8×10^{7}
10^{-8}	1.28×10^{-15}	1.6×10^{6}	8×10^{6}
10^{-7}	1.28×10^{-14}	1.6×10^{5}	8×10^{5}
10^{-6}	1.23×10^{-13}	1.6×10^{4}	8×10^{4}
10^{-5}	1.28×10^{-12}	1.6×10^{3}	8×10^{3}
10^{-4}	1.28×10^{-11}	1.6×10^{2}	8×10^{2}
10^{-3}	1.28×10^{-10}	1.6×10^{1}	8×10^{1}
10^{-2}	1.28×10^{-9}	1.6	8
10^{-1}	1.28×10^{-8}	1.6×10^{-1}	8×10^{-1}
1	1.28×10^{-7}	1.6×10^{-2}	8×10^{-2}

* For a 0.96" x 1.28" area on a 60 microampere/lumen photocathode.

** Assuming that no noise is generated in the image orthicon.

An image orthicon type tube has a target gain of 3 to 5 and a 5-stage dynode multiplier gain of 500-700, totalling about 2500. Thus, for a 5:1 signal-to-fluctuations ratio, this calculation limits minimum scene brightness to about 6×10^{-6}. It is therefore necessary to increase overall tube gain by better photocathodes, use of optical preamplifiers, minification, higher target gain, or higher dynode multiplier gain if we hope to reach lower scene light levels.

4. Optical Preamplification With Minification (Figure 2)

From the study on fluctuation limitations, it is evident that work on decreasing threshold scene brightness should preferably involve increasing the signal from the photocathode of the image orthicon. This could be accomplished by a number of methods. However, only those systems which increase the quanta of available information will increase the inherent sensitivity of the tube. A more sensitive photocathode would be one example, since the present surface has only a 10% quantum efficiency. By use of a larger lens with the same f number, more quanta would be received by a larger photocathode. By minification with a suitable electron optics, the larger number of photoelectrons (information quanta) could be fed to a standard camera tube. An optical amplifier tube which produces minification is in production at Westinghouse. It is known as the Fluorex or x-ray image intensifier type WL5997.

A study has been made of techniques which can be used in fabrication of an image orthicon tube with a preamplification stage such as shown in Figure 3. This structure consists of an image intensifier stage preceding a standard image orthicon tube. The tube as shown consists of a high voltage intensifier minification section having a 4½" diameter photocathode in a 7-3/8" diameter bulb. The output of this section is an aluminized phosphor layer which is almost in contact with an adjacent photosurface on the opposite side of an extremely thin layer of glass. This photosurface will be identical in position and function with the photosurface in the standard image orthicon tube. It was estimated that this preamplifier section should produce a gain of more than 200. We also considered the possibility of eliminating the phosphor layer and the image section of the image orthicon tube, and simply having the electrons from a large photocathode focussed directly on the target-mesh assembly. To obtain the appropriate 400 or 500 volt electron energy, such a structure would probably require a special electron optical system, whereas in the structure of the #520, we were able to utilize the standard image intensifier electron optics. Also, such a low voltage structure would have less amplification and was therefore not considered as desirable.

Figure 2 - Image orthicon with preamplifier. The preamplifier is an image intensifier tube like the type WL5997, physically and optically coupled to the face of the image orthicon.

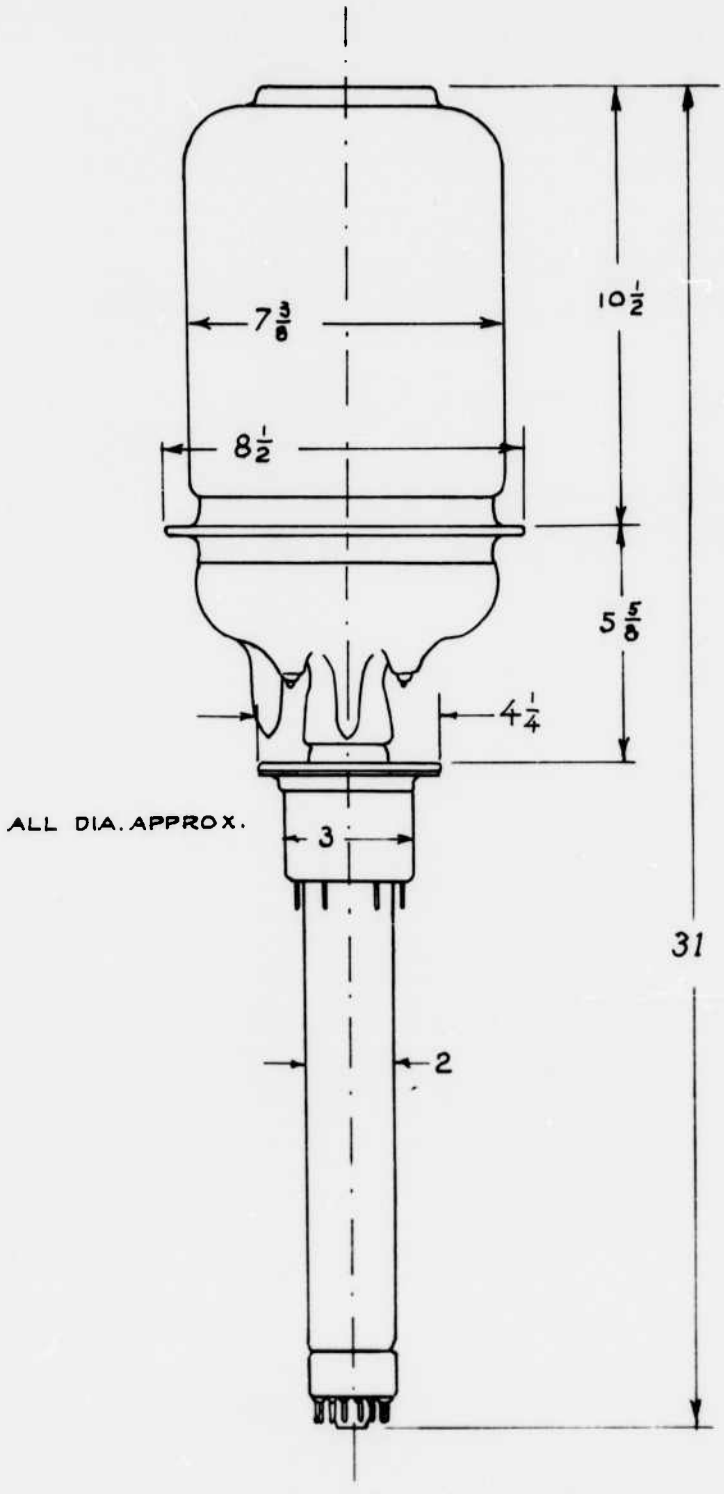

Figure 3. Special Image Tube Outline

Figure 4 shows a typical design curve for the preamplifier stage, which gives the output brightness of the preamplifier stage as a function of input brightness for various gains, ranging from 50 to 10,000. If the complete output brightness is transmitted without loss to the input of an image orthicon tube, as is substantially the case with the integral image orthicon and preamplifier tube, it is possible to predict at least approximately the quality of imaging which will be realized in the combined tube. For 300 lines resolution, 10^{-3} foot candles are required. Thus, with a 1000 power preamplifier tube, it should be possible to image to the order of 300 lines, at 10^{-6} f-c on the preamplifier photocathode. These computations neglect shot noise from the photocathode of the preamplifier. They also neglect background brightness often caused by field emission on the output phosphor of the preamplifier tube. These lines represent preamplifier tubes having output background brightnesses of 5×10^{-4}, 10^{-3}, and 3×10^{-3} f-c respectively. It is evident that if the background brightness of the preamplifier is above the output signal, the latter will be masked. Thus, if the amplifier in the above example had a background of 3×10^{-3}, then the output signal at 10^{-6} photocathode illumination would be completely submerged in background brightness and the image would start to appear at about 3×10^{-6} f-c on the input photocathodes.

It is seen that if background brightness can be completely eliminated, the threshold of the combined tubes for a gross image will not be lowered indefinitely, but will be limited by the threshold of the image orthicon which will still occur somewhere between 10^{-5} and 10^{-7} f-c. Also, as the light level decreases, the operation of the image intensifier preamplifier becomes limited by fluctuations in the preamplifier photocathode current. Assuming the same 60 microampere per lumen photocathode and the same contrast in the scene to be viewed, the minimum photocathode illumination for reproduction of a picture of a given resolution in a given time will be reduced by the ratio of the photocathode areas. That is, if the theoretical threshold of the image orthicon for 500 line reproduction of a 100% contrast picture in 1/30 second is 4.2×10^{-6} foot candles photocathode illumination), the fluctuation limit for the preamplifier will be about 1/8 of this, or 5.3×10^{-7} foot lamberts scene brightness. This is with the assumption that an f/0.85 lens is used to cover the 2.7" x 3.6" photocathode area of the preamplifier.

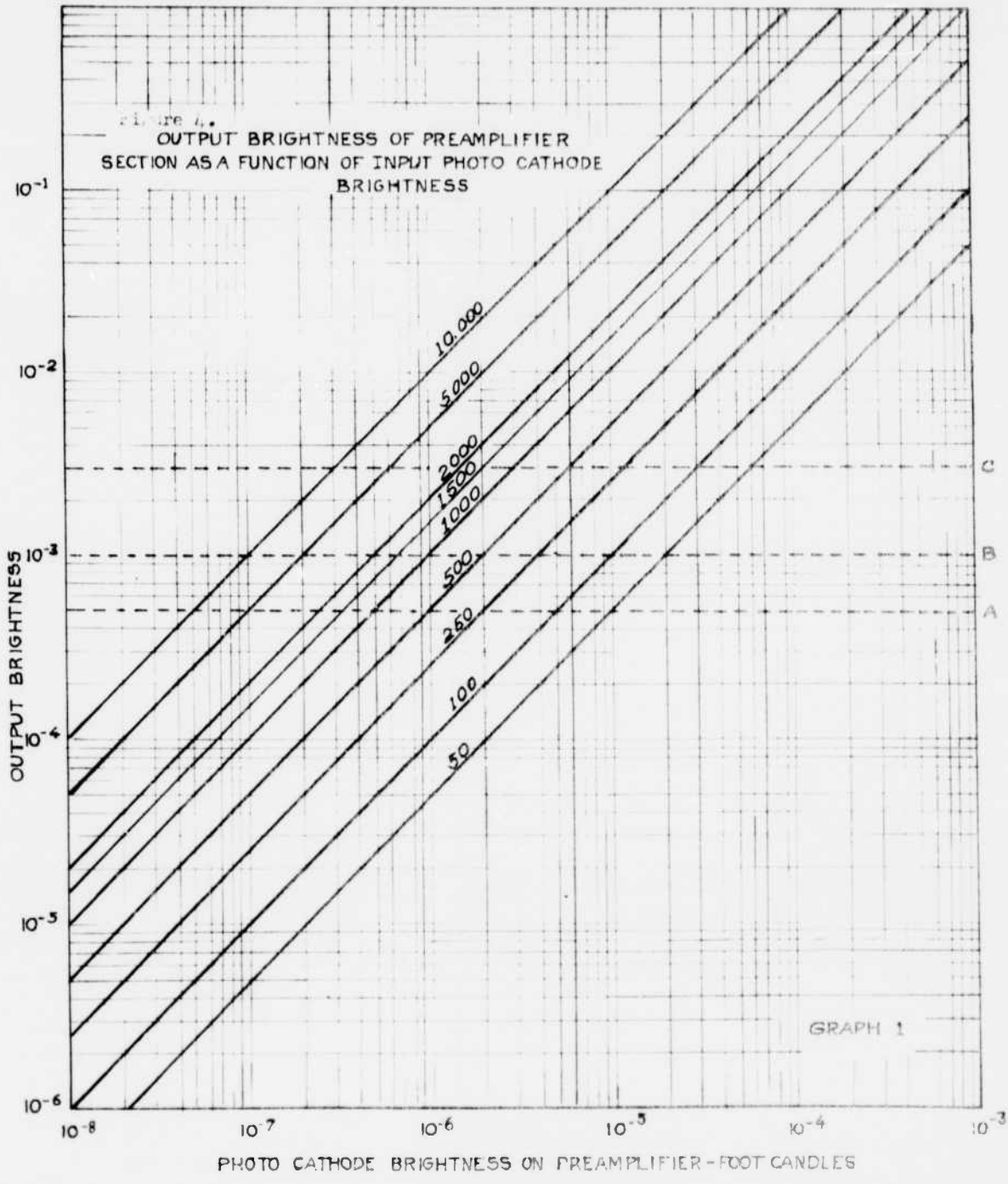
Figure 4.
OUTPUT BRIGHTNESS OF PREAMPLIFIER SECTION AS A FUNCTION OF INPUT PHOTO CATHODE BRIGHTNESS
OUTPUT BRIGHTNESS
10^{-1}
10^{-2}
10^{-3}
10^{-4}
10^{-5}
10^{-6}
10,000
5000
2000
1500
1000
500
250
100
50
C
B
A
GRAPH 1
10^{-8}
10^{-7}
10^{-6}
10^{-5}
10^{-4}
10^{-3}
PHOTO CATHODE BRIGHTNESS ON PREAMPLIFIER - FOOT CANDLES

5 Effect of Target Mesh Spacing on Sensitivity

As the target-to-mesh spacing is increased, the capacitance between the target and mesh decreases, so that stored charge necessary to produce a given voltage charge on the target is decreased. For a standard image orthicon tube using .002" target-to-mesh spacing, the capacitance between the 0.84" x 1.12" scanned area on the target and the mesh is 106 micro micro farads. Many tubes developed under this contract had experimentally observed thresholds at a photocathode illumination of about 1×10^{-6} f-c. For a 60 microampere/lumen photosurface, this corresponds to 5.1×10^{-13} amperes to the target. Assuming a typical target gain of 3, this is a target charging current of 1.53×10^{-12} amperes. In 1/30 second, the system frame time, the target potential on a .002" spaced tube would change $\frac{5.1 \times 10^{-14}}{106 \times 10^{-12}} = 4.8 \times 10^{-4}$ volts.

For a tube with .050" target-mesh spacing, the change in target voltage in 1/30 second would be 1.2×10^{-2} volts, with the same charging current.

The scanning beam in an image orthicon is not mono-energetic, but emission velocity considerations show an energy spread of several tenths of a volt. For near threshold imaging, the highest energy electrons in the beam will land on the target, and a given change in target potential will make a relatively small change in the number which land. Thus, the time required to reach an equilibrium in the target due to the charging current and that portion of the beam current which lands may be several frames or even several seconds for a closely spaced target and very low light levels.

This will limit the ability of the tubes to follow motion or to reproduce rapid changes in brightness. A tube with a wide spaced target mesh assembly will reach equilibrium sooner and should therefore be more satisfactory for very low light level use on moving scenes, although sensitivity measurements made in our lab have not definitely confirmed the theoretical possibility that wide spaced tubes are more sensitive than normally spaced tubes. Use of a more nearly mono-energetic beam would also be desirable to decrease the time necessary to reach equilibrium. This approach is being used on Contract AF33 (616) 3254.

6. Effect of Target Gain

For an image orthicon, the minimum scene brightness for reproduction of a gross image has been shown to be limited partly by fluctuations in the scanning beam and partly by fluctuations in the input stage of the video amplifier. Any means which for a given screen brightness will increase the net signal current to the target will increase the signal-to-beam fluctuations ratio. Any factor which will increase the overall gain of the tube will increase the signal-to-video amplifier fluctuations ratio. Considerable attention was therefore paid to means for increasing the signal gain at the target.

A signal gain is produced when the secondary emission yield of the target for the 400 to 500 volt photoelectrons is greater than 1, provided that the collector mesh is more positive than the instantaneous target potential. Measurements were made of the signal gain at the target in the standard tube. In this case, the surface of the 0083 glass is probably coated with a thin layer of cesium and oxygen deposited when the photocathode is formed. As described below, various special coatings were applied with intent to increase the secondary emission yield.

Calculations were made of the efficiency of the collector mesh for the secondary electrons. This is, of course, a function of the instantaneous target-to-mesh potential. Through field plots with a target-mesh potential of 2 volts and by use of trajectory plotting for the secondary electrons, it was estimated that the present 64% transmission 500 conductor per inch mesh collects 40-50% of the electrons leaving the target. The remaining 50-60% describe parabolic paths in the field between the mesh and the photocathode and are turned back toward the target. Another 40-50% are intercepted by the mesh on the return trip. The remaining 25% pass through the mesh and are redistributed on the target.

These redistributed electrons with energies below the first secondary emission crossover for the target charge the target negatively, causing a black edge or halo around brightly illuminated areas. The redistributed electrons with high energies, above first crossover, may charge the target positively, causing a white halo at a greater distance from a very brightly illuminated area. It was shown that the redistributed electrons will return within a distance of .008"/V of their point of origin. Some electrons will have energies up to those of the 400 volt primary electrons and may therefore land anywhere on the target.

If the electron collection efficiency of the mesh could be improved, slightly higher target gains could be realized. It was theorized that use of a thicker collector mesh of the same optical transmission would collect oblique secondaries more efficiently, and hence should help to reduce the undesirable halo effects described above. This approach is being followed in Contract AF33 (616) 3254.

B. Experimentation to Determine Feasibility of Items Shown Promising

1. Improved Target Storage

One method considered for obtaining usable images from lower light level scenes is to turn off the scanning beam and let the charge image pattern accumulate on the target over several, or many, frame times. In practice, this produced very real gains in contrast but had limitations since the resolution increased only slightly, and did not show the resolution expected from the

higher amplitude target signal. As explained in the introductory theoretical section, most of the factors limiting threshold imaging in the image orthicon occur when the signal is removed from the target or in the subsequent amplification processes. Therefore, if storage were perfect, one would expect that threshold light levels could be made to give 500 line resolution provided that the product of the threshold photocathode illumination times the storage time in frame times, equaled the photocathode illumination required to give 500 line resolution in continuous imaging. In practice, the maximum resolution obtained in stored images, never exceeded about 200 to 250 lines and was always below the curve of resolution vs. light level for continuous imaging, if one substituted for light level the product of threshold light level times the number of frames stored.

We have performed two sets of tests. To separate the effects of leakage through the volume and across the surface of the target from other factors which might prevent the tube from accumulating a stored image perfectly. In the first, the tube is continuously exposed to a very low light level scene and after a varying number of frame times storage, the target is scanned once, having the beam current and other camera controls set for optimum imaging under these conditions. Typical data at various light levels for a standard tube demonstrates that while the quality of imaging does increase with increased storage time, the percentage increase is not what would be expected. The second type of experiment turns off both the scanning beam and the monitor kinescope. The tube has been previously adjusted for optimum imaging on a knee light level scene, but is now operating in a dark room with the camera aimed at a test pattern. A flash of light of sufficient total energy to charge the tube to the knee is allowed to fall of the test pattern. There is then a controllable delay time after which the tube and monitor kinescope are scanned for one frame. This we have called the "retention time" of the tube. The quality of the retained image is studied and to make this test quantitative, we have defined a retention product which is the product of the retention time in frames multiplied by the resolution in the observed picture. During the course of this contract, we have performed these two tests on tubes using the standard Corning 0083 glass target, also on tubes using a similar glass target but with special surface treatments to attempt to increase the surface leakage on tubes using special higher resistance glass targets, and on tubes using anistropic targets, that is, targets made of relatively high resistance glass containing a matrix of conducting plugs to effect metalic conduction through the target. The latter were made from Corning type C photoform glass which has a volume resistivity of 10^{16} ohm centimeters. Because of the variation of volume resistivity of the glass target with temperature, one would expect the retention to be less effective at higher bulb temperatures. At normal operating temperature of the image orthicon in a camera,

that is, between 35 and 50°C, the storage quotient, that is, the number of lines resolution times the seconds storage time for standard image orthicons, ran between 15 and 135. The average retention product was about 50 for standard tubes. Attempts were made to increase the retention capabilities of the tube by special surface treatment of the target glass to increase surface resistivity. Targets were given special treatments as detailed below.

Targets were given special sulphuring treatments to reduce sodium ion concentration at the surface of the target and targets were etched to increase the length of the leakage path across the surface of the target. None of these means increased the retention product for a tube by more than a factor of 2 or 3 compared to a standard tube. In comparison, a tube made with a target of photoform C glass with metal plugs had a retention product of the order of several thousand, whereas some of the other tubes stored so poorly that after one second the picture was unreadable. The photoform target tube retained up to a 123 line image after a period of one minute, to give a retention product of over 7000. As indicated above, the storage performance of the photoform target tube was not comparable to the outstanding retention. The relative storage ability of photoform to specially treated standard glass did not vary of more than a factor of 2 or 3. This data indicates that leakage through or across the target is probably not the dominant factor in limiting the storage ability of an image orthicon.

Tests on various type tube structures have, in many cases, shown much improvement in retention, but in every case there has been no proportionate improvement in storage. There are quite a number of factors which could cause these results but the exact cause or causes have not been isolated.

The results of these two sets of experiments appear to indicate that the failure to accumulate a charge pattern at the expected rate cannot be explained on the basis of surface or volume resistivity alone but is probably due to the redistribution of the electrons or to induced conductivity or stray spurious signals, or thermionic emission originating at the photocathode.

Because this mechanism may ultimately be connected with those factors which prevent lower light level imaging in the image orthicon, we are making further studies of this effect on the current contract AF33 (616) 3254.

A description of our various experiments designed to produce anisotropic target in which conductivity through the target was far higher than lateral conductivity follows.

a. Silver Diffusion Techniques and Results

Silver was evaporated onto a standard image orthicon target, approximately at 400°C. There was no noticeable increase in conductivity through the target. A number of targets were then prepared by evaporating silver through a fine mesh to produce a dot pattern on the surface. These were air-baked for 17½ hours at 400°C. The target showed a definite increase in conductivity in the region covered with silver dots as compared to the parent glass. Note that large area electrodes were used and no attempt was made to prove the conductivity around individual dots. A target was then prepared with a silver polka dot pattern using the same bake schedule. The ratio between the silvered and non-silvered areas was about 35:1 by probe measurement. Glass slides .006" thick were prepared with silver evaporation in register on both sides. With the same air-bake, no improvement in conductivity was evident in any of these sections. The thin targets were then baked for 85 hours at 400°C in an air furnace. When again tested, they showed definite evidence of further silver diffusion. The resistance of the glass beneath the silver surfaces decreased to the order of 10^6 ohms as compared to a value of about 2×10^9 ohms, which had been measured after the 17½ hour bake. The measurements are relatively uncertain because the resistance reading depended on the pressure applied to the probe. In no case was any decrease in resistance noted opposite uncoated areas, where the resistance was of the order of 10^{11} ohms. With the proper baking schedule, it was possible to produce this enhanced conductivity effect, while still preserving a 500 mesh silver structure. Apparently lateral diffusion which occured was not sufficient to obliberate the 500 mesh conductivity pattern in the very thin glass targets. Since our object was to obtain higher lateral resistance, a series of experiments were conducted with higher resistance glass to determine whether the silver diffusion enhanced conductivity effect could be used to decrease the transverse conductivity. Targets of Corning 0120 glass .002" thick were fabricated in the conventional manner. Some targets were silver coated in a 500 mesh pattern while others had 1/4" polka dots. A sample of each was baked for 65 hours at 395°C in air to determine whether enhanced conductivity would occur. Areas which had been silvered showed presence of silver oxide by a yellow stain. However, the glass appeared to have softened in the silvered areas and the 500 mesh pattern showed

considerable lateral diffusion to the point where the pattern was lost completely. No increase in conductivity was obtained. We believe this was due to the fact that the 0120 glass has a relatively small sodium content, approximately 1/4 that of 0083 glass. As the silver diffusion is considered to be a replacement of the sodium, it is possible that there was not enough sodium in the 0120 glass to produce the proper effect. Corning 0010 glass was also tried and gave the same results as the 0120.

b. Increased Target Resistivity by Electrolysis

These experiments were aimed at using standard 0083 glass and increasing the resistivity in selected areas by sodium ion depletion.

The method used was to heat a .006" thick section of glass in an air area at 465°C with electrodes on opposite focus with a 500 VDC potential difference. Measurements were made at definite time intervals for 2½ hours. With continued sodium ion depletion, the glass resistivity increased as was shown by the logarithmic decrease in current with time to 1/8 the original. The voltage was then raised to 750 VDC which gave a current of 380 microamperes after 45 minutes. The glass ruptured when the voltage was raised to 1000 VDC. Examination of the glass showed that there were a number of white dots on the surface under the negative electrode which were analytically determined to be sodium. While this rough experiment was successful, we estimated that the difficulty of making satisfactory electrical contact with the glass in a fine matrix pattern made this approach less advantageous than those described below.

c. Photoform and Porous Vycor Targets with Conducting Plugs

One method of producing a highly anisotropic target is to selectively drill or etch the glass to form a matrix of holes which may be filled with electrically conducting materials. Corning photoform C glass has a volume resistivity of 10^{16} ohms centimeters and can be prepared in the desired form by appropriate photochemical processing. Samples of photoform were obtained in 165 and 300 line per inch mesh pattern. The 300 line mesh samples had a hole size of .0024 inches, separation of .009" between holes and were .007" thick. After several trials, a satisfactory method was determined to fill the holes with conducting plugs of silver powder. The most successful method placed the photoform over a porous stainless steel sheet through which air could be drawn into a vacuum chamber connected to an aspirator. The silver powder was mixed with

e. Increased Surface Resistivity of Target

(1) Cesium-free tube

As a result of materials deposited on the target during the normal tube processing, we felt that the surface resistivity of the target was materially lower than the volumetric resistivity, and therefore a limiting factor in storage ability. One tube was made with a simulated photocathode to investigate whether cesium in the tube might be substantially lowering surface resistivity. Test results showed approximately the same storage characteristics as standard tubes with cesium processed photosurfaces. This led us to believe that cesium has relatively little effect on deterioration on the storage characteristics of the standard tube.

(2) Etched Target Surface

In an attempt to increase the lateral resistance, etching was used to increase the leakage path length. Both vapor and solution etching and frosting was tried with hydrafluoric and ammonium bifluoride solutions. Considerable difficulty was experienced, particularly at the glass seal of the targets. No substantial improvement in storage or retention was measured.

(3) Evaporated Thin Films on Target

A tube was made with a calcium fluoride coating on the target evaporated in two strips—light and heavy. Storage and retention ability were about the same for both strips and not much better than standard. In addition to calcium fluoride, targets were made with evaporated strips of MgF_2, Al_2O_3, SiO, and SiO_2. The "bloom" process was also used. This is a process which exposes the glass at the annealing temperature to a sulphur dioxide atmosphere so that the sodium at the surface of the glass reacts with the sulphur dioxide of the atmosphere around it and produces soluble sodium sulphates. These may then be washed off leaving a silica enriched or sodium depleted surface. We found no significant improvement in storage or retention.

f. Effects of Temperature on Retention and Imaging

The image orthicon, its yoke and assembly, were placed in a box packed with dry ice. This made it possible to take measurements over the range from 115°F to -75°F. In general, the retention appeared to increase at lower temperatures,

presumably due to increased target glass resistivity. Light levels for threshold imaging decreased slightly as temperature was decreased below normal operating temperature. Threshold then rose, probably due to inferior imaging ability at the lower temperature values. At the lower temperature values, the signal was very degraded due to increased target glass volumetric resistivity.

2. Increased Target Gain

Theoretical calculations show that it should be possible to increase the ability of the image orthicon to operate at lower light level scenes if the secondary emission yield from the target could be increased. Targets were coated with a discrete dot pattern of antimony dots in the expectation that an array of cesium antimonide dots having a known high secondary emission ratio would be formed at the same time that the photocathode was made. These tubes showed no improvement in target gain. Other surface treatments included calcium and magnesium fluoride evaporations, the sulphur bloom treatment mentioned above, and fabrication of the target from a thin film of silicon monoxide evaporated across the open areas of a 500 line mesh. None of these showed any increase in target gain.

3. Target Gain Measurements as a Function of Illumination

Data indicates that the effective secondary emission ratio of the target varies substantially with photocathode illumination increasing to relatively high values for low light levels. We believe that this effect is due to a considerable extent to the decreased collecting field between the target and mesh as the target charges positively. At the light level of the knee, the target gain is approximately 2; at 1/4 of the knee light level, the ratio increased to 3.3; at 1/10 of the knee, the gain was 4-5; at very low light levels, our measurements showed target gains as high as 30-50. Whereas, the accuracy of these very low current measurements at near threshold light levels is not great, there is a definite increase in gain for lower light levels which may be attributed to the more efficient collection of secondaries as the light decreases.

4. Additional Gain Provided by Dynode Multiplier Stages

In section A3, Camera Tube Signal Amplification Requirements, it was shown that for very low light level imaging under the assumptions of the 60 microampere/lumen photocathode, a gain of 3 in the target and a gain of the order of 500 for the dynode multiplier structure noise in the first stage of video amplification would set a lower limit for seeing.

To eliminate amplifier noise as a limitation at the scene brightnesses at which we are now working, it is required that the overall gain of the camera tube be increased by a factor of ten or more. To provide this gain, shown to be absolutely essential by the calculations, we have built several tubes using two additional dynode multiplier stages. Although this amplification is not as effective in obtaining lower thresholds as would be higher gain earlier in the tube, say in the photocathode or in the target, it should be effective if amplifier noise is actually a limiting factor. The best tube to date, which incorporated a 50 mil target-mesh spacing, photocathode sensitivity of 60 ua/lumen, and a total dynode gain of 10,000, gave a threshold picture at 2.37×10^{-7} f-c on the photocathode. This is the most sensitive camera tube made during the course of this contract and represents a sizable increase on prior art tubes. Data on the secondary emission yield of silver magnesium multiplier surfaces vs. voltage of the primary electrons show a broad maximum at 400-500 volts per stage. Slight improvements in threshold have also been obtained by increasing the usual 1250 volt supply for the five stage dynode multiplier to 1850 volts and adjusting the voltage across the individual stages for optimum resusts. These tests confirm that additional dynode gain effects a substantial increase in camera tube sensitivity. In view of our calculations on the effect of overall tube gain, it seems probable that the high target gains measured at low light levels must be approximately accurate since otherwise the standard 5 dynode tube would not image satisfactorily at 10^{-6} f-c on the photocathode.

5. Electron Bombardment Induced Conductivity Approach

This work has been done at the Westinghouse Research Labs in E. Pittsburgh with the aim of developing an entirely new sensitive optical amplification device. In this tube which is described in Figure 5 electrons from a photocathode are accelerated through 12-30 kilovolts, focussed, and made to strike a thin target consisting of a support layer, a conductive layer, and on top a layer of a substance which is made conductive by bombardment with high energy electrons. Among satisfactory substances for this target is pure selenium. Various methods could have been used to scan the selenium target in order to make use of the electron bombardment induced conductivity effect to generate an image. In the interests of simplicity, and because extremely high gains may be obtained with this target, it was decided to use vidicon type scanning. The operation of the scanning section of the tube is therefore similar to that of the standard 6198 vidicon, and the video signal developed is taken out from the conducting backing layer on the BIC target. Initial selenium target tubes showed objectionable persistence which was overcome by using selenium of extremely high purity. During the course of this

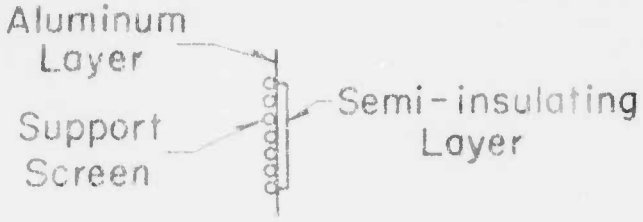

Enlarged and Exaggerated Section of Target T

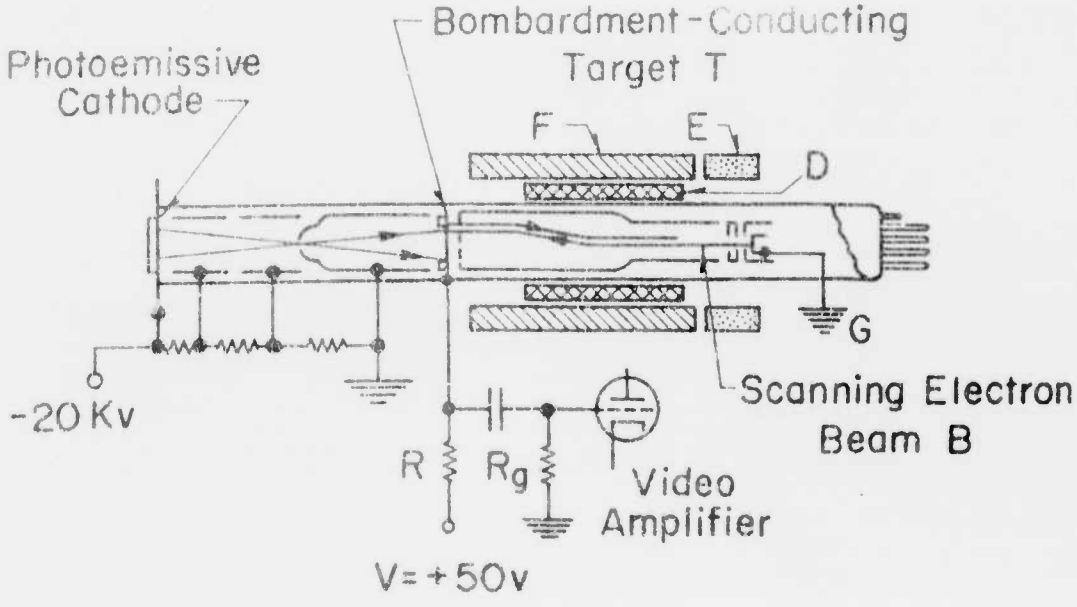

Figure 3. Ebicon

contract, operable ebicon tubes were made which gave usable images at 0.37 f-c photocathode illumination. Principle problems encountered were stray leakage and field emission due to presence of cesium in the high voltage image section and the difficulty of obtaining a satisfactory photosurface. The photosurface yield on the tube mentioned was only 0.2 microamperes/lumen. Extrapolating from the small vidicon photosurface to the size used in an image orthicon and to the photosurface sensitivities found in image orthicon practice, this tube would have given an acceptable picture with a photocathode illumination of 8×10^{-4} f-c. Work on the ebicon is continuing under the current contract AF33 (616) 3254 with the emphasis on work to obtain higher gains in the electron bombardment induced conductivity target. If gains of 1000 can be realized in this target, the ebicon may exceed the sensitivity of the best present day image orthicons, even with the vidicon type scanning system which does not include a dynode multiplier stage.

6. Image Intensification by the Use of Mesh Control Grid for Storage of Image

This approach was considered at the beginning of the contract, but no experimental work was done as we preferred to take advantage of work being financed by the Air Force at other companies on storage devices. Work done at Farnsworth on Signal Corps contract DA36-63073 and DA36-039SC-42310 indicate that a threshold of 10^{-6} f-c photocathode illumination might be obtained but only with a very long storage time of about 8 minutes. The general conclusion from the study of the data was that it would not be worthwhile to pursue this avenue in view of more promising approaches.

C. Conclusion - Discussion of Results of Phase A

The operation of both standard and experimental tubes at low light levels has been investigated and the factors effecting threshold have been evaluated. This evaluation of results is more simple if the tube is divided into three parts—the photosurface, target, and scanning section. We will consider these three as separate entities for the moment.

1. Photosurface

A tube made with silver bismuth oxygen cesium photosurface has shown a threshold of just over 10^{-7} f-c. The best approach to increasing the sensitivity of the tube is to improve the photosurface. However, this is also the hardest approach and no significant gains were made under this contract.

The use of a larger photocathode provides more quantum information. By use of a 25:1 high voltage minification image section, an improvement in threshold of about 4.5 was demonstrated. This was limited by field emission in the preamplifier due to the high voltage necessary to produce minification.

A third method bypassed, but did not overcome the quantum limits. By storage, the effective sensitivity was increased, at the expense of time resolution. However, storage does not improve the inherent sensitivity of the tube, and emphasis was shifted from this work in order to permit continuous rather than intermittent viewing. It was possible by the use of storage to improve the resolution by a factor of from 2 to 4. This, in effect, improves the threshold by the same factor.

2. Target Gain

It is necessary to produce a certain voltage on the target to obtain a viewable signal. With a previously determined photocathode current, attempts were made to increase the target gain to produce a larger charge. It was demonstrated that the target gain varies as a function of illumination. Thin films evaporated on the target to produce higher secondary emission yields did not show significant increases over the standard target. This was probably due to the presence of cesium compounds which were formed during sensitization of the photocathode. A maximum target gain of 50 was recorded at threshold. This is about 5 times the average value at threshold. The disposition of a thin film of silver on the scanning side of the target showed average improvement of 2 in threshold due to reduction of fluctuations when the scanning beam hit the target.

3. Scanning Section

It was shown that a major present limitation on low light level operation of the standard image orthicon is the inherent fluctuation signal associated with the scanning beam. With standard tubes, this was calculated to limit the threshold to about 10^{-6} f-c photocathode illumination, and verified experimentally. Much of the above described work was aimed at increasing the signal on the target to override the fluctuations in the scanning beam. By increasing the gain of the multiplier section of the gun, a photocathode illumination threshold of 2.37×10^{-7} f-c was obtained. This was the lowest threshold obtained on any experimental tube made under this contract.

The work done on this contract has indicated the most fruitful approaches to increase in sensitivity. Gains effected by reducing the beam noise and improving the dynode multiplication will be limited. These gains, though limited, will be necessary. The greatest improvements will be effected by increasing the photo-

cathode current. The obvious method would be to increase the photocathode efficiency, as this will add to the available number of information quanta and improve the operation of the entire bulb. The next best approach is to amplify the photocathode current before it hits the target.

The efforts put forth on this contract have shown a definite improvement in the threshold by extra dynode multiplication and by image preamplification. The avenues of approach which promise the greatest improvement in sensitivity are being put into practice under the present WADC contract AF33 (616) 3254.

III. Phase B - Microphonics

A. Theoretical Calculations

1. Vibration Data on Modern Aircraft

To determine the magnitude of the problem of designing a non-microphonic image orthicon, we obtained data on vibrations in modern aircraft in the range from 0 to 600 CPS from report No. 120X-7, March 30, 1951, by North American Aviation, Inc. For reciprocating engine aircraft in flight, acceleration due to vibration are generally less than 3G except in the following locations: the engine nacelle, outer wing and tail structures. For jet engine aircraft, the points which are above 10G represent vertical vibration during flight in the fusalage, tail section, tail structure, and outer wing panel. Except for these locations, accelerations of most points in the aircraft lie below the 5G line. Therefore, a camera tube which would operate well at accelerations up to 3G would be useful in many locations in reciprocating engine aircraft and a tube which would operate at 5G would be useful in jet engine aircraft. Further information was obtained from out Westinghouse Lima Works covering the vibration spectra in the B-52 in the range up to 2 kc. There are areas in the plane, for example, the crew compartment, for microphonics where a 5G threshold for microphonics would be satisfactory. There are other areas where 10 and 15G thresholds would be necessary.

2. Vibration Data on Prior Art Image Orthicons

Vibration data taken on image orthicons made just prior to the start of Phase B of this contract showed that standard commercial image orthicons available at that time displayed perceptible microphonics at average accelerations below 1G in the range from 65 to 450 cycles/second. Acceleration at higher levels not only seriously degraded the performance, but caused tube failures attributed to open heater leads and broken targets. The upper limit which the prior art tube would stand without permanent damage was approximately 5G.

3. Type of Microphonics Effects

We have found that the chief source of spurious (microphonic) signals during vibration of the image orthicon is the relative motion of the target and mesh, which results in an oscillatory change in the capacitance between them. Since the potential of the target is fixed, the capacitance change causes a target voltage change which represents a spurious signal to the scanning beam. The appearance of these microphonics is similar to a horizontal bar pattern superimposed on the video signal. The width of the bars is fairly constant across the picture but the number of

bars visible in one frame time is a function of the frequency of vibration. The intensity rather than the number of black bars is a measure of the target mesh microphonics, no matter what their exact cause.

The second cause of microphonics in the tube is directly attributable to the gun and dynode assembly. Studies of gun vibration show that the cantilever construction of the gun and multiplier section allows considerable displacement during transverse vibration. These microphonics can be observed and separated from target mesh microphonics by biasing the target negative so that the beam will not land on the target. While gun microphonics may also appear as horizontal black and white lines, the gun microphonics are easily distinguishable since they persist when the target is cut off. The width of the black lines is often only two to four scanning lines , or they may appear as very wide light and dark bands as much as 1/4 of the raster height in width.

While the type of microphonic effects described above degrade the performance of the tube during vibration, they themselves are not the cause of permanent tube damage. There are other results of vibration such as cracked stem fillets, broken welds or breakage of the target which have caused complete failure in standard image orthicons. These are also considered microphonic effects, and are necessarily treated under this phase of the contract.

At the beginning of Phase B of the contract, it was recognized that some at least of the microphonics found in tube testing were due to relative motion between the coils in the focus and alignment-deflection yoke assembly and to weakness in the tube mounting. Work in other laboratories was therefore concentrated on this aspect and has resulted in an improved coil assembly and tube mount which became available and was used for tests made in the last few months of this contract.

Theoretical Calculations

1. Basic Theory of Target Mesh Microphonics

A diagram in cross section of the principal elements of the image orthicon appears on page . Electrons from the illuminated areas of the photocathode are accelerated toward and focussed on a .0002" thick 1.4" diameter glass membrane called the target. For these 400 volt bombarding electrons, the secondary emission ratio of the target surface is about 5, and the resulting secondaries are collected by a very fine copper mesh placed close to the target on the photocathode side and maintained slightly positive with respect to the target. The photoelectrons thus result in the accumulation of a positive charge pattern on the target in which the more positively charged regions correspond to brighter parts of the picture. The opposite side of the target is scanned with a focussed beam of very low velocity electrons, from a cathode whose potential

is chosen so that the beam electrons with maximum emission velocity can just reach the target. Those which fail to land are returned to an electron multiplier to form the output signal from the tube. As this beam scans over a part of the target which has a larger positive charge, more electrons land on the target, and fewer are returned to the multiplier. This modulation of the return beam, varying from point to point in response to the potential of the target, and resulting from the positive charge pattern and hence from the illumination pattern, constitutes the video signal.

To allow for collection of secondaries through a suitable target voltage range at higher light levels, as the photoelectrons charge each part of the target in the 1/30 of a second between scans. The collector is usually operated 2 volts positive with respect to the lowest value at which beam electrons will land on the target (target cutoff voltage). During most or all of each frame time, the target is negative with respect to the mesh by 1 or more volts. For very dim scenes, where very little positive charge is accumulated between scans, the average target mesh potential difference may be nearly 2 volts.

In prior art image orthicons for entertainment purposes, the spacing between the target and mesh was only .002" to .003". Now, how do microphonic signals arise? The capacitance between the scanned area of the target and the mesh is about 110 micro micro farads, the applicable formula being that for a plane parallel capacitor $C = Ko\ A/d$, where $Ko = 8.85 \times 10^{-12}$ farads per meter in the Meter Kilogram Second system of units.

During operation, this capacitor carries a charge corresponding to a 1 or 2 volt target-mesh potential difference. During vibration if the target and mesh move with respect to each other, the target mesh capacitance will change, and since the charge is essentially constant, and since the mesh potential is fixed by the circuit, a change in instantaneous target potential will result. If the relatively negative target moves toward the mesh, the capacitance will increase, the target will become more positive, and more of the scanning beam will land as it would have in brighter parts of the picture. If the relative vibration frequency of target and mesh is a few hundred cycles, a dark and light horizontal bar pattern should appear superimposed on the picture.

Note that the effective frequency of this bar pattern will be the sum of the frequencies of the target and mesh, which will in general be different. Because of the many possible modes of vibration for each, many different exciting frequencies may be expected to excite target-mesh microphonics. The presence of microphonics for exciting frequencies below the fundamentals; however, indicates that higher harmonics are being generated either in the machine, the yoke mounting, or through motion of other parts within the tube.

Since the average target mesh potential is approximately a volt, a .001" instantaneous change in spacing during vibration on a tube with a .002" target-mesh spacing, will change the target voltage by 1/2 volt corresponding to a fairly bright bar. To determine how much motion can be expected from typical targets and mesh assemblies and to establish approaches for reducing target mesh microphonics, the following analysis was made:

2. Circular Membrane Theory

A membrane is a skin considered to have no bending stiffness, stretched at such a great tension that increments of tension resulting from small displacements normal to the surface are relatively insignificant. The tension is considered to be uniform. Vibrations of a circular membrane may take place in many modes. In the simplest mode, the center moves with maximum amplitude and the only nodal points lie in the rim, which is fixed. In higher modes, there may be concentric modal circles or nodal diameters or both. The frequencies of the higher modes are not integral multiples of the frequencies of the lower modes. Although the vibrations of such a membrane are not truly sinusoidal, a sinusoidal approximation may be used which gives useful results.

In terms of the mode numbers, where N is the number of equally spaced nodal diameters and S is the number of concentric nodal circles, the frequency of vibration , neglecting damping, is given by

$$f_{n,s} = \frac{A_{n,s}}{2\pi} \quad \frac{1}{R} \sqrt{\frac{S}{m}} \qquad \text{Eq. 1}$$

where $A_{n,s}$ is a constant, depending on the mode, which for the basic (o,1) mode is 2.404

R is the radius of the membrane in cm

S is the tension in dynes per cm across any line in the membrane

M is the mass per unit area of the membrane

In the case of a complex vibration, such as that produced by impact, several modes of vibration may be excited simultaneously. Analysis shows that the total energy of vibration is equal to the sum of the vibration energies of the several modes treated separately and that damping acts on all of them equally, damping all at the same ratio.

For an impulse excited membrane, the displacement at any point y is given by:

$$y = y_o \, e^{\frac{-c}{2\pi R^2 m} t} \cos q(t - t_o) \qquad \text{Eq. 2}$$

where $q = \frac{R n_s}{R} \sqrt{\frac{S}{M} - \left(\frac{C}{\pi A_{n_s} M}\right)^2}$ Eq. 3

which for very small damping reduces to

$$y = y_0 e^{-\frac{c}{2\pi R^2 m} t} \cos\left\{\frac{a_{n,s}}{R}\sqrt{\frac{S}{m}}\,(t-t_0)\right\}$$

eq. 4

in agreement with the frequency computed from equation 1.
Where Y_0 is the initial amplitude of vibration of the point
C is the damping constant in $\frac{\text{dyne sec}}{\text{cm}}$ where F damping = cv

t = time in seconds

The natural logarithm of the ratio between successive amplitudes one period apart is called the logarithmic decrement,

$$\delta_e = \frac{c}{2M} T$$ Eq. 5

Where $T = \frac{1}{f}$ = the period of vibration and M is the effective mass of the membrane. If δ_e and t are known by observation, and the effective mass M is known, c may be calculated from

Eq. 6

$$c = \frac{2\delta_e M}{t}$$

Energy Considerations

For frequency W, where $W = 2\pi f$, and $Z(r, \theta)$ = maximum displacement of the membrane at the point (r, θ) and the motion is represented by $z = z_1 \cos \omega t$, the stored energy is

$$E = \frac{m\omega^2 z_1^2}{2}$$ Eq. 7

where m is the effective vibrating mass at the point (r, θ)

Now, for a circular membrane $W = \frac{A_{ns}}{R} = \sqrt{\frac{S}{M}}$ and $W^2 = \frac{A_{ns}^2}{R^2} \frac{S}{M}$

To calculate E for a given mode, one must integrate this expression over the membrane, since z will vary from point to point. Equation 7 in its present form however indicates that for a given amount of energy imparted to a membrane, the amplitude will be smaller if the resonant frequency is higher.

With damping $\frac{dE}{dT} = -\frac{C}{M} E$ or $\frac{dE}{E} = -\frac{C}{M} dt$

For rapid damping, the damping coefficient c should be large, and the effective mass of the system small. For a forced vibration assuming a sinusoidal driving force accelerating the membrane mount with an acceleration G:

$$y = \delta_{ST} \frac{1}{\sqrt{\left(1-\frac{\omega^2}{\omega_{n,s}}\right)^2 + \frac{4\left(\frac{c}{m}\right)^2\omega^2}{\omega_{n,s}^4}}} \sin(\omega t - \alpha)$$

Where δ_{ST} = the statical deflection under a constant acceleration
G = the peak value of the applied acceleration.

$W_n = A_{ns} \frac{1}{R}\sqrt{\frac{S}{M}}$ = the resonant angular frequency

α = the phase angle

The reciprocal square root expression is known as the magnification factor. When W, the driving frequency, equals W_{ns}, the resonant frequency, the first term in the radical vanishes. If the damping force c were zero, the displacement of y would become infinite. To keep the vibration amplitude small at resonance the damping should be as large as possible for a given mass and the statical deflection as small as possible for a given mass. Since δ_{ST} has the form $\delta_{ST} = \frac{Gm}{R}$, δ_{ST} *, this requires that the tension be as high as possible for a given mass/unit area in the membrane.

* is given by $z(r,\theta) = z(r) = \frac{980 M G(R^2 - r^2)}{4S}$

where R = radius of mesh in cm.
r = radius from center of mesh to distance
m = mass per unit area of membrane
s = tension of membrane in dynes/cm
G = acceleration in G's

At the center of the mesh $r = 0$ and $z_{max} = \frac{980 m G R^2}{4S}$

In the foregoing it is shown that damping does not alter the ratios between the coefficients of individual frequencies. In other words, all frequencies are damped at the same ratio. Damping is therefore a characteristic function of the membrane parameters and not the mode of vibration. From this work, it can be shown that undesirable vibrations can be reduced by several means. An increase of the damping factor of the material is an effective alteration of parameter. Any mechanism which will absorb energy of motion from the membrane, converting this to heat energy, will effectively damp the vibration. Energy is probably absorbed in increasing the thickness of the membrane if the tension is increased proportionately, is one way to increase the damping, as will the use of softer materials.

3. Application of Theory to Mesh Microphonics

It has been established experimentally and theoretically that microphonics in the image orthicon result largely from variations in the target-mesh capacitance. Since the change in capacitance is proportional to the change in target-mesh spacing, it is desirable to reduce the target and mesh vibration amplitudes as much as possible.

According to the preceding section, the amplitudes can be reduced by increasing the damping factor and decreasing the statical deflection for a given acceleration. The latter requires use of higher mesh tension without increase in mass. Standard image orthicons now use .00016" thick 500 wire per inch electroformed copper mesh, with 64% open area whose conductor size is .00040" x .00016". The ultimate tensile strength for this mesh is 130 grams weight/cm. Special image orthicon mesh assemblies in finished tubes made under this contract have been measured to have a tension of about 40 grams per centimeter, 1/3 of the ultimate strength and about 2/3 of the elastic limit. To increase this tension will apparently require use of high strength materials.

The table below gives the natural frequencies for the 0, 1 fundamental mode and statical deflections for various mesh materials we have considered. Tension at 1/3 of the ultimate strength is assumed.

	S Tension Gm/cm	M Grams/ cm	R Mesh Radius cm	Resonant Freq. CPS	Microns Per G
Present Copper Mesh	40	.001	1.78	1350	.197
Electroformed Nickel 500 Mesh	53	.00084	1.78	1690	.126
Woven 304 St. S. Drawn Wire	2460	.0124	1.78	3000	.04
Parallel Tungsten Wires	16 gm		1.75	2530	.048

It is shown from these figures that both woven stainless steel mesh and drawn tungsten wire offer possibilities for great improvements.

in mesh microphonics because of high strength-to-weight ratios which permit mounting at higher tensions. Details of experimental techniques devised to obtain high tension collector mesh assemblies are given below.

4. Application of Theory to Target Microphonics

The image orthicon target type 0083 glass membrane of 1.600" diameter, and from .0001" to .0002" thick, mounted on an alloy ring of 51 per cent nickel and 49% iron. Figure 6 shows the geometry of a standard mounted target in cross section. As originally made, the target is cut from a handblown glass bubble and laid across the target ring, which has been previously painted with solder glass. Ring and target are placed in a furnace and heated to fuse the solder glass and soften the target. Under the influence of surface tension the thin glass membrane is pulled tight and remains so as target and mesh are slowly cooled to room temperature, since the coefficients of expansion of the glass and metal are closely matched.

The target tension is positively established during assembly of the target-mesh assembly, as shown in figure 7 , by deflecting the target with the annular aluminum spacer, which also sets the distance between the target and mesh. The standard 5820 uses a .002" thick spacer. The deflection of the target, however, is the sum of the spacer thickness plus the "dropoff", the difference in height between the outer and inner parts of the mesh support ring minus the height of the solder glass bead above the plane of the undeflected target (see figure 8). Higher target tension, up to the rupture point, may be attained by increasing the amount of deflection.

Typical target tensions for the standard .002" spacer and standard "dropoff" average about 45 grams/cm. For an average target thickness of 0.00015" or .00038 cm, and a glass density of 2.47 grams/cubic cm, the mass per unit area of the target is 9.65×10^{-4} grams/sq cm. The free area within the aluminum spacer is about 1.4" diameter (3.56 cm). The resonant frequency of the target is, therefore

$$f_{01} = \frac{2.404}{2} \quad \frac{1}{R} \sqrt{\frac{S}{M}}$$

$$= \frac{2.404}{2} \quad \frac{1}{1.78} \sqrt{\frac{45 \times 980}{9.65 \times 10^{-4}}} = 1460 \text{ cps}$$

The statical deflection is described by

$$z(r,\theta) = \frac{980 G m \left(R^2 - r^2\right)}{45}$$

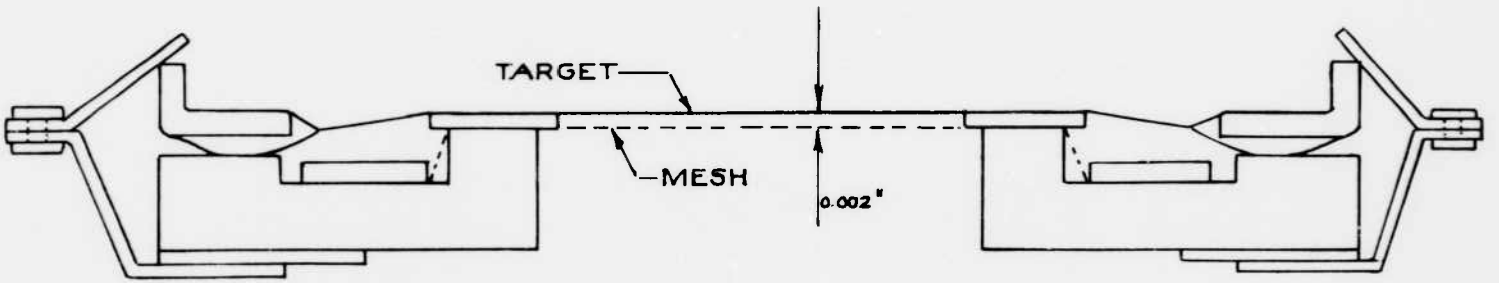

Figure 6. Geomtrey of a Standard Mounted Target in Cross Section.

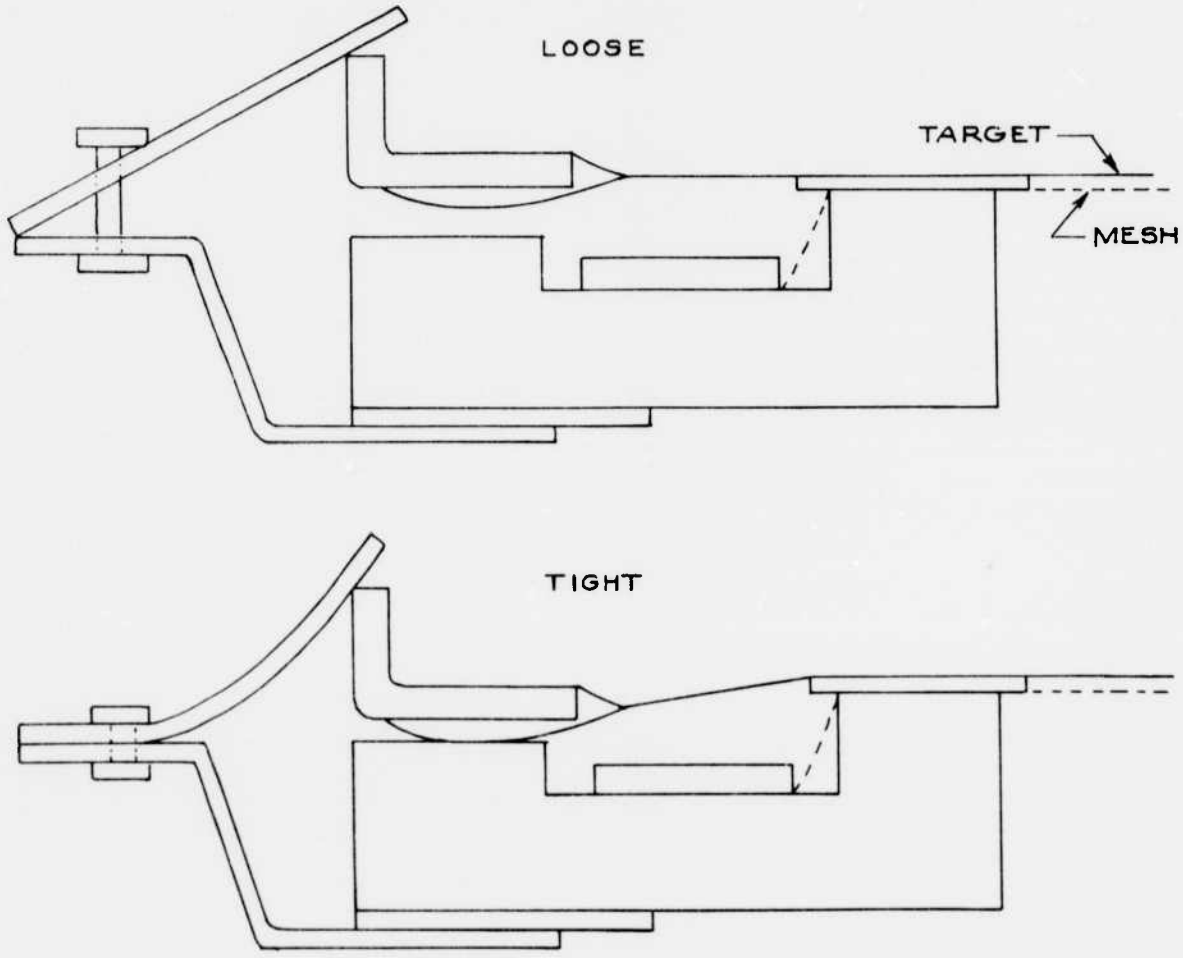

Figure 7. Target Mesh Assembly.

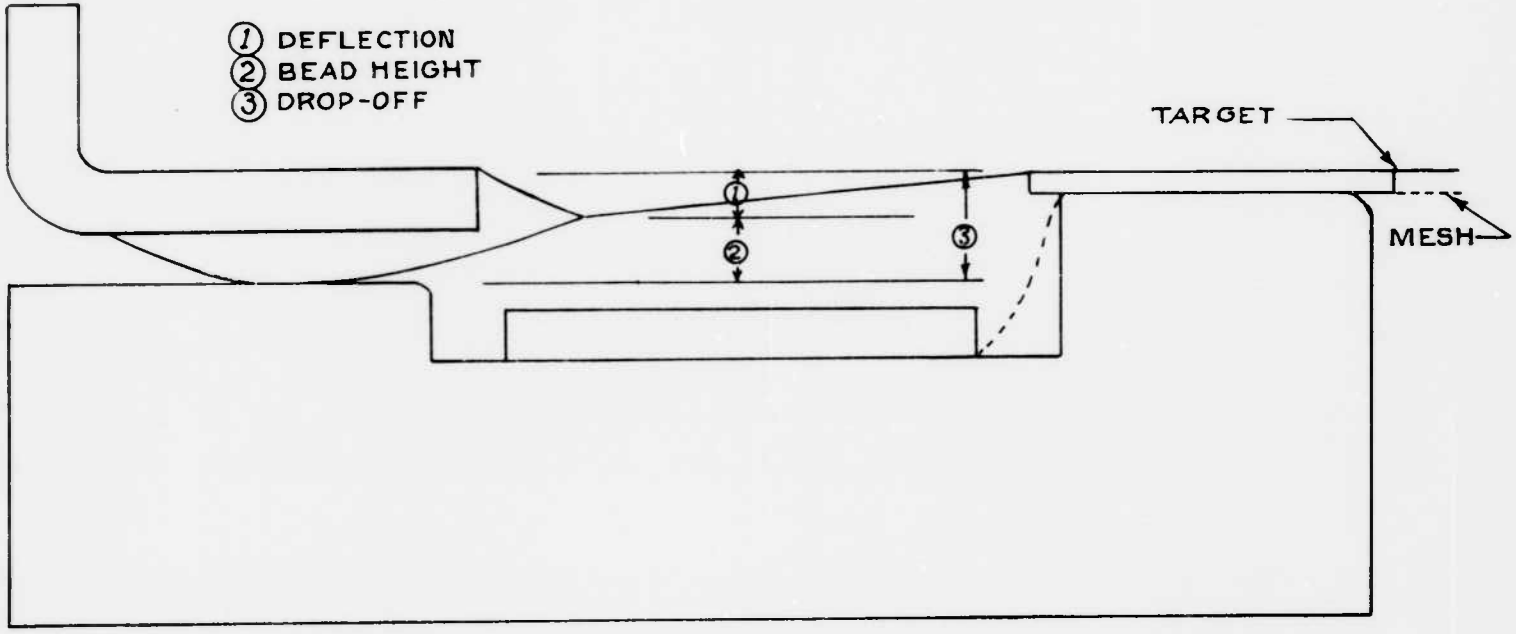

Figure 8. Deflection of Target.

The maximum center deflection per G acceleration is therefore

$$\frac{Z_{max}}{G} = \frac{980 m R^2}{4S} = \frac{980 \times 9.65 \times 10^{-4} \times (1.78)^2}{4 \times 4.5 \times 980}$$

$$= 1.7 \times 10^{-5} \text{ cm or } 0.17 \text{ microns}$$

During the course of this research, means were devised to increase target tension about 10 times. This increases the resonant frequency in the fundamental mode to 4600 cps and decreases the statical deflection to .017 microns.

5. Damping

For rapid decay of microphonics induced by impulses, and to keep vibration microphonics small at resonance, the damping factor should be as large as possible. Damping in the present target and mesh assembly seems to be very slight, since impulse excited microphonics in the standard tube often persist for seconds. Damping of such a membrane vibrating in vacuum probably takes place through relative motion of the outer fibers in the glass or mesh which convert the energy to heat. This relative motion is probably greatest at the rim where the membrane is rigidly supported in cantilever fashion.

Greater damping could therefore be caused by use of a thicker target or thicker mesh, provided that the tension is increased proportionally in which the relative motion of the extreme fibers will be greater for a given deflection. This effect could be heightened by use of materials with high internal damping. Alternatively, the mesh or target could be greatly increased in thickness, as through the use of photoform for the target, and mounted as a thick disc to decrease deflection and increase damping in vibration.

C. Experimental Evaluation

1. Target-Mesh Microphonics

a. Wide T-M Spacing

As the target-mesh microphonics have been shown to be a direct function of the change of capacitance between the membranes, the most direct way to decrease the percentage change in capacitance would be to separate the membranes as far as possible. The T-M microphonics did become less critical in experimental tubes as the spacings were increased to the order of 75-150 mils. As the spacing is increased from 25-50

mils, the quality of imaging appears to go through a maximum. Above that distance, the quality of image decreases. 100 mil spacing was determined to be the best compromise spacing. As an extreme case, a tube was made with no collector mesh in the hope that the target support cup would serve as a collector. This tube did not image.

b. Integral or dot spacers

Another way to decrease relative motion between the target and mesh during vibration is to apply restraints between them at points which are normally not nodes. In the extreme version the target and mesh functions should be fulfilled by one integral member. The first evaluation of this approach was made accidentally.

High frequency sparking on tube #75 caused the mesh to be attracted to and remain in contact with the target. While there were certain areas where contact was not made, a sufficient portion of the target and mesh did stick together to permit studying the effect of contact. In these portions, no T-M microphonics were evidenced. There was a very substantial time lag due to the extremely high capacitance of the tube. This discouraged additional tubes on integral assemblies which would have high target-mesh capacitance, although several ideas were put forth and tried experimentally to determine that a fine mesh pattern could successfully be evaporated on a target

To overcome the disadvantage of high capacitance, a tube (#119) was made with 3 discrete areas of the target-mesh assembly fastened together by dots of colloidial silica and zirconium. Tests of this tube showed no improvement over the standard tube; however, we believe that the adhesive failed to bond to the glass target. Other adhesives, such as kasil, showed that they tend to break the target.

c. Smaller target and mesh

As can be shown from the theoretical considerations, decreasing the membrane area is one of the most effective parameter changes. Several tubes were made using wide target-mesh spacer rings with only the rectangular raster area open in the center. This decreased the vibration area of the target and mesh from a 1.4" diameter wide to a rectangle. (1.12" x .84") Tube #114 was made with this type spacer and a normal .002" T-M spacing. The microphonic performance was slightly above average and the duration of microphonics unusually short. Tube #184 incorporated a 1/2" diameter

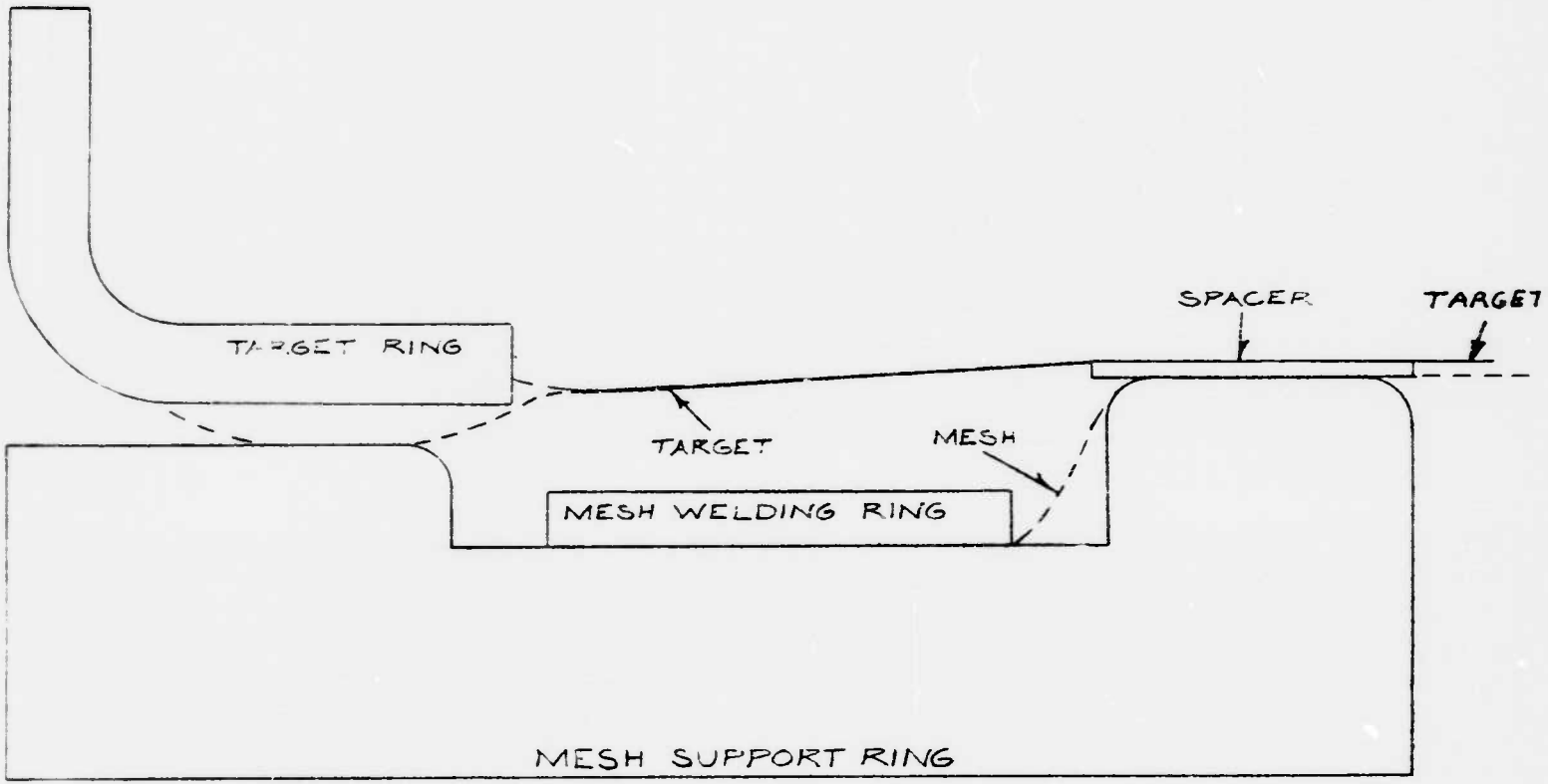

Figure 9. Sectional View of Image-Orthicon Target-Mesh Assembly.

target and mesh area with a standard spacing. There were no narrow-band type T-M microphonics.

d. Higher tension mesh and target

(1) Target

From the theoretical calculations mentioned previously and experimental results to determine the ultimate strength of the target, it was possible to calculate what deflection of the target by a concentric ring spacer was necessary to produce a satisfactory level of target tension which would not break the target during processing. As a result of this work, it has been possible to increase the tension of the targets by a factor of 10 over the tension normally obtained using the standard T-M assembly. This increase in target tension has been made possible to a large extent by the development of a technique for nondestructively measuring the tension of the mounted targets. Observations of target tensions before and after exhaust bakeout indicated that there is relatively little loss is target tension during tube processing.

The increase of tension was accomplished primarily by increasing the target deflection, but special structures were found necessary to accomplish this satisfactorily. Greater deflection effected by stacking standard spacer rings have broken targets at 50% of the experimentally determined yield point. This was found to be due to rapid curvature of the target over the spacer, where the target glass was bent 5° in .001" along the glass. A special spacer assembly was designed to reduce this curvature to 0.5° per .001". Use of these spacers permitted tenfold increase in target tension without excessive breakage in tube processing.

(2) Mesh

(a) Standard 500 mesh copper

Tests run with the normal 500 line copper mesh show that the ultimate tensile strength is about 3 times the normal tension in a tube. A tension figure of 40 grams/cm has been taken as standard and the ultimate tensile strength is about 120 grams/cm. The present mounting technique is to lay the mesh on a flat sheet of copper which has a groove for the mesh support ring (see figure 6), which is figure 1 of Floyd's memo in March 1956 report.)

The mesh is pulled smooth by the operator's fingers, the mesh welding ring is pushed down into place and spot welds made around the ring. This technique produces a moderately smooth mesh, but allows variations in tension from area to area in any one piece, as well as variations between assemblies. This irregularity is evened out during a subsequent firing schedule, during which the mesh is tightened by baking at 800°C for a short time. The best theory consistent with experiments of how the mesh becomes taut involves the recrystalization of the electroformed copper mesh and a phase change in the steel support ring. It can be assumed that the mesh has a net overall tension of approximately zero when it is spot welded to the steel support ring. Between room temperature and 200°C, there is a loosening of the mesh due to the difference in coefficients of thermal expansion between the steel and copper. Between 200 and 750°C, the copper begins to recrystalize and contract and will become flat again at close to zero tension. Between 750 and 800°C a phase change occurs in the steel, resulting in a contraction of the ring. If the mesh is allowed to continue recrystalization, it will overcome the slackness due to the contraction of the ring and become flat again at zero tension. On the cooling cycle, there will be a sharp increase in the ring size due to the phase reversal, with a corresponding increase in mesh tension. Further increase will be obtained from the differential contractions of the mesh and ring from this point to room temperature. This theory is consistent with results of firings done at 600 and 700°C, below the phase change point, which show tensions below normal. The use of other materials confirmed this theory. Kovar and Carpenter Invar #36 rings, which have no phase change, were fired with resultant tensions far below normal.

Past a certain minimum firing time, there appears to be no further increase in tension. Times from ten minutes to 1/2 hour gave comparable results. With the normal schedule, the final tension is limited by the strength of the copper at the temperature (625-675°C) at which the phase reversal phase change occurs in the steel support ring.

In order to eliminate the variation in initial tension due to the present mounting techniques, as well as the uncertainty and losses during firing, it

would be advantageous to mount the mesh at the desired final tension and eliminate the firing schedules in present use. A tensioning device has been made in which the edge of the sheet of mesh is clamped tightly with a rubber "O" ring. A smaller "O" ring then presses the mesh into a groove larger than the target support ring in the lower plate of the fixture, stretching and tightening the mesh. By this means, mesh have been welded with tensions of 45-50 grams/cm against 40 grams/cm average for the field mesh. However, even with very fine control, the yield before breaking of the copper mesh is so small that experiments with mechanically tensioned mesh were discontinued as impractical with this type fixture.

Measurement of the tension of standard mesh which had been subjected to the heat treatment of subsequent tube processing during sealing and exhaust showed that there was a definite loss during the process. While the finished mesh is taut at room temperature, it looses tension and becomes quite wrinkled at tube bakeout temperature (375°C). This, with the comparatively low temperature of the bakeout indicated that creep in the material under stress is not a factor. Standard 5820 mesh are aluminum flashed on the target side before installation to prevent spotting the target during exhaust when the mesh may be slack enough to touch the target. To investigate the possibility that a reaction of aluminum with the copper may be involved we made tubes in which the standard aluminum evaporation on the mesh was eliminated. This gave the desired effect, as there was no significant loss of tension during the processing of these tubes. Since most non-microphonic tubes have wide target mesh spacing, the mesh does not touch the target during exhaust, and aluminum flashing is unnecessary.

(b) Use of stronger mesh materials

Electroformed nickel mesh has higher tensile strength than electroformed copper, but the percentage improvement is not very significant. After preliminary experiments, nickel mesh was discarded. The use of mesh woven from drawn wire affords substantial possibilities increase in tension for a given mass per unit area. For 400 mesh stainless steel with .001" wires, 1.25 grams/sq cm and 36% optical transmission wire, it is possible to obtain 18700 grams/cm ultimate strength. This compares to 130

grams/cm for the present 64% transmission electroformed copper mesh weighing 0.1 grams/sq cm and 157 grams/cm for the available 60% transmission nickel mesh weighing 0.084 grams/sq cm. If each mesh is stressed to 1/3 of its ultimate strength, this gives a tension to specific mass ratio of 400 for the copper, 590 for the nickel, and 4800 for the stainless steel.

Based on calculations, we find that the wire diameter of the woven mesh must be reduced to the order of .0004" to prevent visualizing the mesh during operation, and to obtain equal optical transmission.

To evaluate use of this mesh experimentally, we at first attempted to etch the wires to reduce their diameters. It was found, however, that acid etching to such fine dimensions left the wires non-uniform in diameter, and wire breakage resulted. We then tried electropolishing or deplating experiments which showed that the wires can be reduced uniformly to almost any desired diameter.

A fundamental difficulty associated with etching or deplating woven mesh has proven to be loosening of the mesh and lateral movement of the wires, resulting in uneven wire spacing. This unevenness, if uncorrected, is great enough to appear in the video image. To prevent this movement of wires, it was necessary to produce constant tensions over the entire mesh by means which can pull the wires straighter as their thickness decreases. The use of the jig mentioned above, which was unsuccessful in producing mounted mesh tension with electroformed copper mesh, worked admirably in this case. Five tubes were successfully made with 400 mesh stainless steel electropolished to the desired wire diameter.

An investigation was made of the commercial availability of fine woven wire mesh with the proper wire diameter and spacing, of stainless steel, molybdenum, or tungsten.

The only sample obtained during the course of this contract was woven of .7 mil molybdenum wire at 250 wires per inch. A single piece 4" x 4l" was received. However, the supplier declines to weave more of this mesh at this time. The sample was received in the last few days of the contract and has not been evaluated. Work done under the contract shows that coarser mesh patterns can be used with no loss in resolution in a tube with .100" t-m spacing.

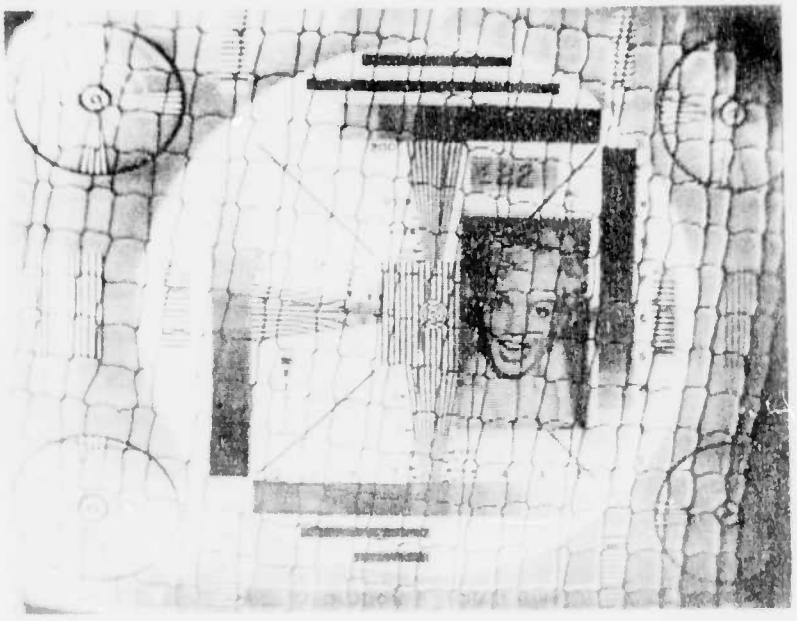

Figure 10 - This photograph shows a monitor view of tube #122 which had a piece of dynole mesh used as a target mesh with a T-R spacing of .010". It illustrates the imaging quality of such a tube and points out the visibility of large (.002") wire when used for target mesh.

(c) Stretched Wire Grids

As an alternate approach, experimental image orthicons were made with stretched parallel wire collector grids. In tube #155, 12 wires of .0007" diameter were stretched diagonally under varying tensions across the raster area at an average target-mesh spacing of about .005". This tube produced a picture crossed by diagonal dark lines, the image of the individual wires exployed. (Figure 8).

Bright bands on both sides of each wire are probably related to the high target element capacitance between the wires and areas of the target immediately under them. This target wire capacitance may be expected to drop off rapidly for target elements at increasing distances from the sides since the wire to wire spacing was about .050", compared to .005" wire to target spacing. Through redistribution, the potential of the target just before scanning is probably fairly uniform. The bright bands would thus represent the higher charge signal accumulated on the higher capacitance elements of the target. The collection efficiency of this grid is probably relatively low, which would increase the redistribution of low energy secondaries to other more positive parts of the target and so serve to minimize potential differences. The bright areas may also be explained on the basis of more efficient collection from the target areas immediately under the wires.

If the above theory is right, the difference in signal between the bright bands and darker areas of target between them may in a sense be considered to visualize the target grid capacitance pattern.

Figure 9 shows microphonics in tube #155 under very heavy impact. In this photograph, it is evident that areas of the target which are far from a given section of the collecting wires, exhibit relatively small microphonics effects. This effect is very evident visually on the monitor at lower levels of impact where the microphonic effects are confined to the bright areas only. In a sense, tube #155 permits direct visualizing of the benefits of

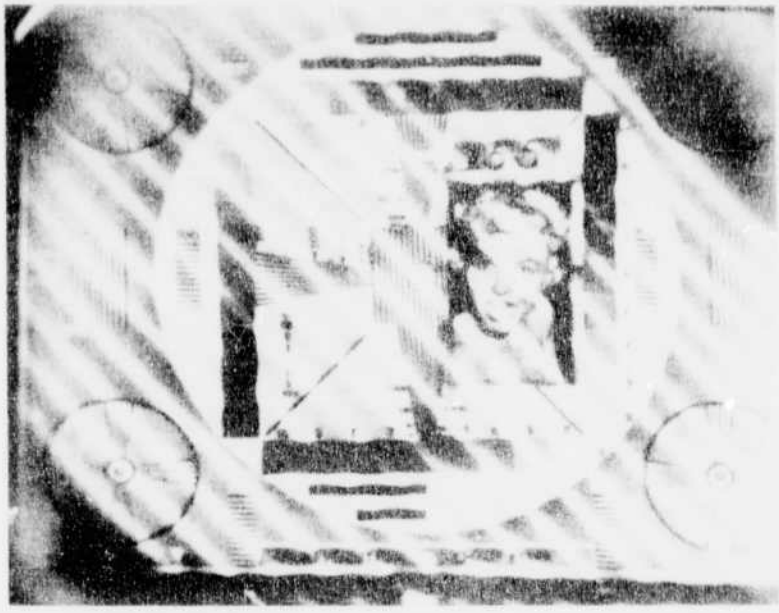

Figure 11 - Stretched wire grid tube #155 with .005" IM spacing, showing visibility of .0007" wire, white border along the wires and imaging between wires. The tube was not under vibration when this photograph was taken.

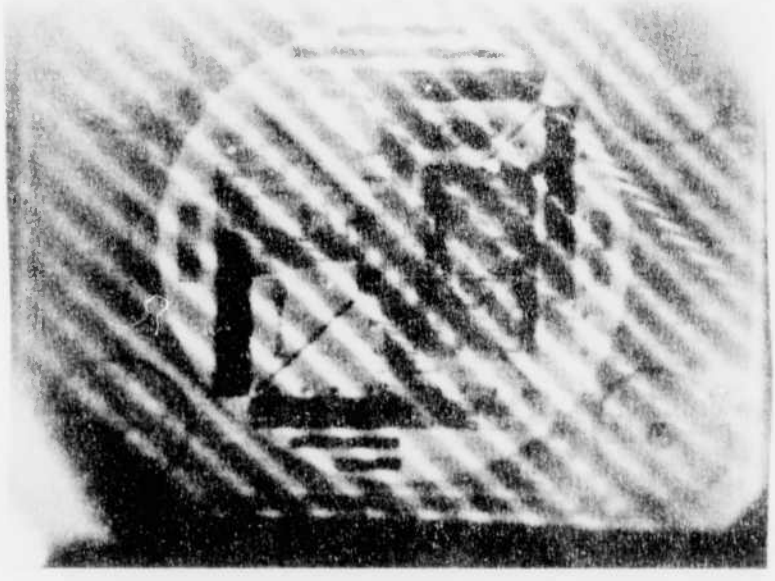

Figure 12 - Stretched wire grid tube #155 showing appearance of image when the tube is subject to impact. Note the different frequency and intensity of the vibration of various wires. These wires were mounted with varying tensions.

wider T-M spacing, although the geometry of the grid is sufficiently different to prevent an exact comparison. The microphonics also appeared to definitely relate to the tension and length of the individual wires which were intentionally mounted with varying tension. This may be considered experimental verification of the improvement which should be associated with a smaller area target-mesh assembly and tighter mesh.

The individual wire technique afforded an excellent opportunity to study in one tube the effects of T-M spacing. 600 line resolution was obtainable in the relatively large areas on the target between mesh wires. As the T-M spacing is increased, the inter-element capacity of the raster becomes predominant, and the role of the T-M capacitance decreases. The indications are that white areas on the tube #150 visually represent the T-M spacings where the T-M capacitance plays the more important role; the dark areas where inter-element capacitance predominates.

As shown in photograph 5, the anti-microphonic benefit of wide T-M spacing corresponds to a condition where the maximum T-M capacity under vibration is still small compared to the inter-element capacitance. The white high signal areas on tube #150 do not show up in standard tubes having 500 mesh and close T-M spacings. Since the distance between conductors is above equal to the T-M spacing.

Late in the contract year, a machine-wound grid of 1/2 mil wire, 20 mils from center to center was attempted. It was determined by preliminary tests that this grid is entirely feasible and that high uniform tensions could be obtained. It was further determined experimentally that for wide target-mesh spacing of the order of 050" to .100", the mesh will not appear in the image. However, this project was shelved to concentrate in the remaining time on obtaining more complete vibration with the recently received M.B. vibration machine.

2. Gun and Cathode Microphonics

The standard 5820 image orthicon exhibited some microphonics even while the target was biased negatively. While significant, these are a second order effect compared to the T-M microphonics, and must be considered to be gun or circuit microphonics. The latter

were eliminated since the microphonics disappeared when the beam was cut off. In general, gun microphonics are caused by any vibration which tends to modulate the scanning beam, particularly that which changes the spacing between the cathode and cathode grid or which moves the defining aperture in the screen grid out of alignment with the beam crossover, as well as any vibration which alters the position of the gun defining aperture sideways with respect to the target. The latter, if severe can cause a vibrating shift of the televised image which we have called image flutter.

A tube was set up external to the yoke, to experimentally locate the microphonics of the gun structure by monitoring the current from the cathode to G1, G2, G3, and G4 and on an oscilloscope observing the percentage change in the steady stage currents due to the vibrations. Some of the tubes showed a very substantial change in the beam current under this test. However, no correlation was found between these tests and the imaging microphonics as seen on t the monitor.

Five types of gun microphonics were observed on the monitor. 1. Alternate light and dark streaks 2-4 lines wide. 2. Wide light and dark bands, whose width was sometimes 1/4 of the raster height. 3. A series of very bright dots followed by trailing black streaks. 4. Very bright narrow streaks, about 2-4 lines wide. Of these four types of microphonics, it was determined that the latter two are primarily due to contact sparking between the tube and the socket. These have been eliminated by use of a more rugged coil and tube-mounting assembly. 5. Waviness of the image. This slow waving distortion of the image was entirely different from the T-M microphonic effect and was probably due to a lateral movement of the gun assembly.

To overcome the microphonic effects of the gun section we built experimental tubes with means to prevent the gun from moving with respect to the tube envelope and means to prevent relative motion between parts of the gun and dynode multiplier assembly. As a first attempt, a tube was made which incorporated a heliarc welded kovar ring at the base of the gun to support the entire cathode assembly. This experiment gave some promise. We found more promising an experiment to eliminate the canteliver mounting of the entire gun assembly by welding kovar buttons to the G3 electrode, which were then sealed to the glass envelope of the tube, providing a firm support for the entire assembly at G3, in addition to the present support by the stem leads. Additional support was provided by using double bulb spacer springs between the G4 ring and the tube wall. This version worked well and was used in most tubes made near the end of the contract. To prevent motion between the dynodes, ceramic spacers have been incorporated between each dynode stage so that the entire gun section may be tightly compressed

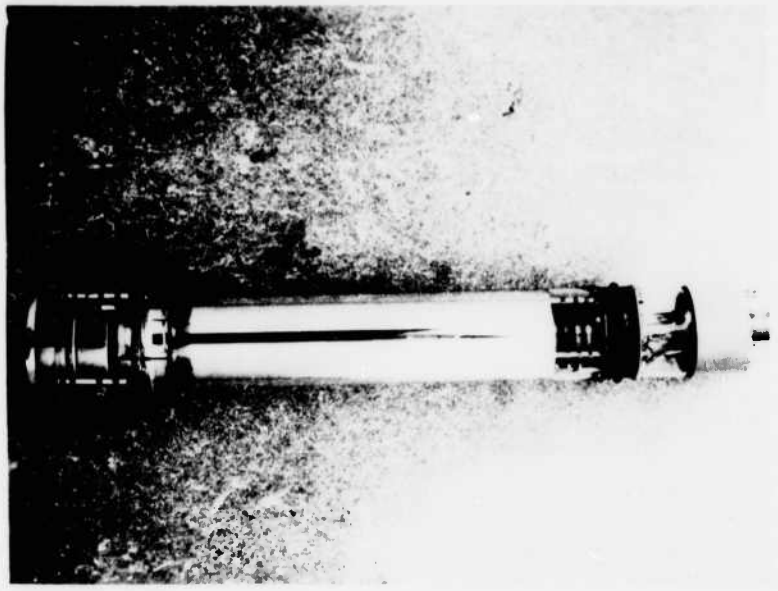

Figure 13 - Tube #143 with kovar ring gun support

Figure 14 - Westinghouse tube type WX3604 showing kovar button gun support.

and welded in place with no lateral movement possible between parts. Several experimental tubes were made with no anode mesh. An extra pinwheel multiplier was added and the current was collected by using the dynode #5 plate as an anode. The change in microphonic characteristics was not significantly great; however, no deterioration of image quality was observed with the anode mesh removed. To eliminate the possibility of sparking at the G4 spring contacts, a tube was made with a G4 painted contact in the image section. This tube showed no difference in gun microphonics. To increase the rigidity of the dynode multiplier section, extra ceramics and clamps have been put on wherever practical, especially to tie down electrode leads which might otherwise strike the gun. We have also substituted an RF getter for the standard electrical getter.

3. Image Section Microphonics

The original image mount was supported cantilever fashion on 7 stem leads. This mounting allowed relative motion of the image section lens cylinders, together with flexing of the stem leads which broke small glass chips from the fillets around the image stem lead seals. Any loose particles in the tube may, during vibration, strike and break the target and mesh, thus effectively destroying the tube.

In order to decrease the strain put on the image stem leads by the cantilever mounting, bulb spacer springs were added to the G6 electrode which were similar to the springs used on G4. Additional ceramics and clamps were used to improve the rigidity of the structure itself. The photocathode contact was moved to allow the use of the stiff nichrome lead directly to back a rigid bulb contact for the photocathode. The most difficult problem has been in obtaining a fillet around the leads which is properly re-entrant so that no feather edge of glass exists to be broken off by lead vibration. To avoid these feather edges, the leads are made of kovar within the seal but welded to a nichrome lead which does not seal to the glass. The nichrome is further painted to avoid direct glass contact. Extreme care in the stem-making operation and possibly some additional development work will be required to obtain a reasonable yield of good stems.

D. Methods of Testing

1. Ball Drop Test

After experimental work on different means of impact testing, the following was accepted as the standard impact test. A 9/16" diameter steel ball weighing 11.9 grams was dropped through a steel

tubing onto the base of an image orthicon tube. The column was arranged so that the height of the ball drop was adjustable from 1" to 12". The microphonies could either be observed visually or, where more detail and accuracy was required, by photographing the monitor with an arrangement which synchronized a camera shutter with the impact of the ball.

It was found that the microphonic frequencies observed from the impact test were of the order of 900-2500 cycles/sec. For an 11" drop the accelerations were estimated to be over 10G.

2. Continuous Vibration

A. Acoustic Coupling

This method used a loudspeaker placed close to the tube. The speaker was driven by an audio-oscillator. In these preliminary tests it was demonstrated for the first time that the microphonies on a given tube go through periodic maxima and minima as the frequency is varied. In general, a rough agreement existed as to the frequency of the audio-oscillator and the frequency of the microphonies as determined from microphonic bars on the raster, and from observation with an oscilloscope.

b. Mechanical Vibration Table (8-55 cps)

As the loudspeaker method of producing continuous vibration gave accelerations which could not be easily measured and required painfully high sound levels, work was continued using an All American vibration machine with an eccentric and Scotch yoke driven table. This machine covered the frequency range from 9-55 cycles/second with a constant amplitude. However, the accelerations actually applied to the tube may have been higher than those calculated because of harmonics or lost motion in the machine. Comparison between results using the ball drop test and the vibration table appeared to indicate that the ball drop test was somewhat more severe than 10G vibrations on the vibration table at 50 cycles. Fixturing was designed for the vibration table so that the tube could be vibrated both perpendicular to the tube axis (Y axis) and parallel to the tube axis (Z axis). However, the same jig was used initially for both longitudinal (Z axis) and transverse (Y axis) vibration, and it was determined that this arrangement was not sufficiently rigid and subjected the tube to more than the rated acceleration values.

c. MB Electromagnetic Exciter (5-2000 cps)

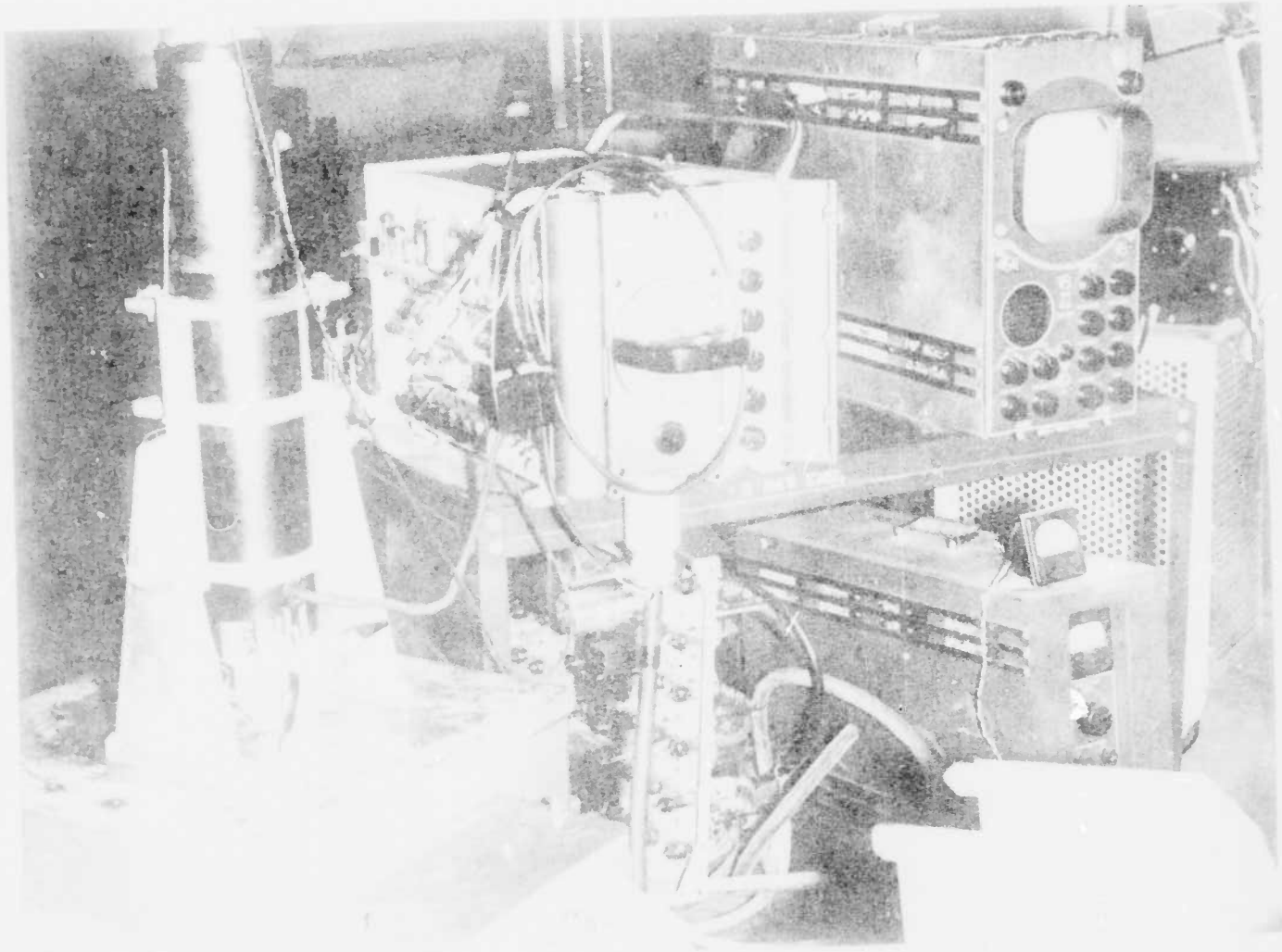

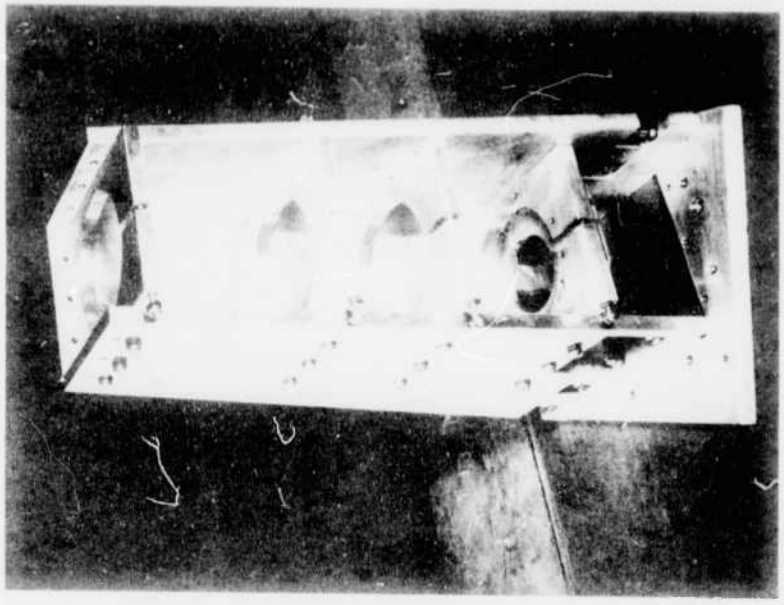

Figure 4. - Vertical, Z axis, mount for use with MB electromagnetic vibration exciter.

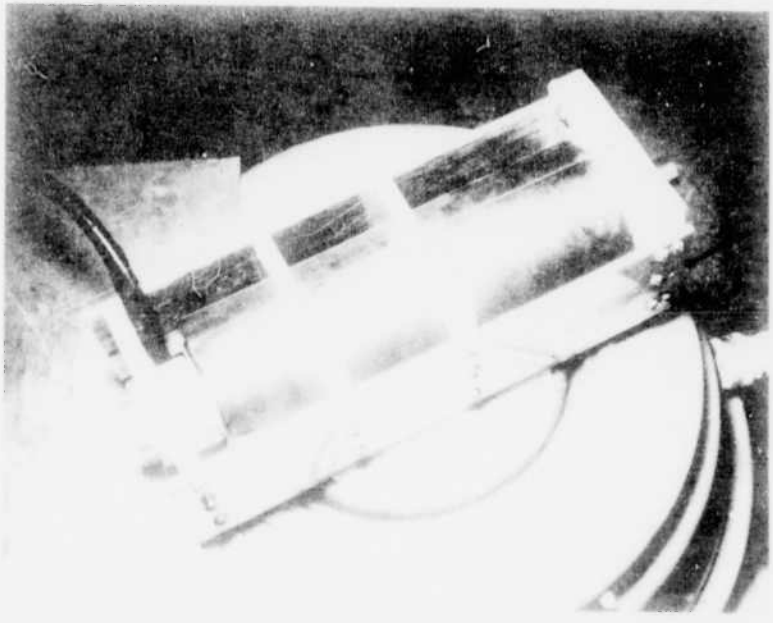

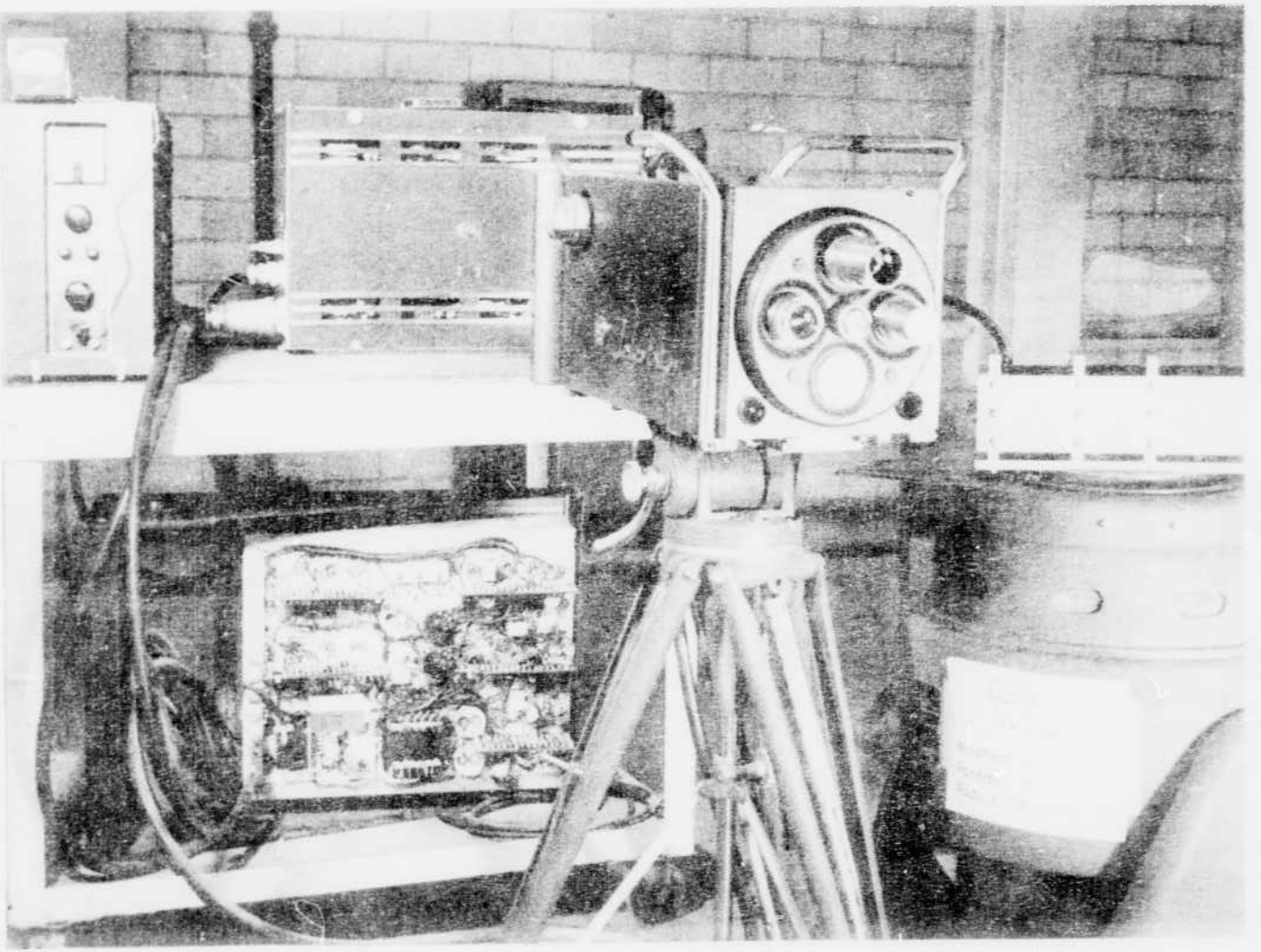

Figure 6. Equipment used with the MB electromagnetic vibration exciter. On the table: power supply, camera control, and monitor. The sync generator is on the bottom shelf. The TV camera is in the center. At right is the vibration table with horizontal yoke mount in place. At the far right is shown the electronic control unit for the exciter.

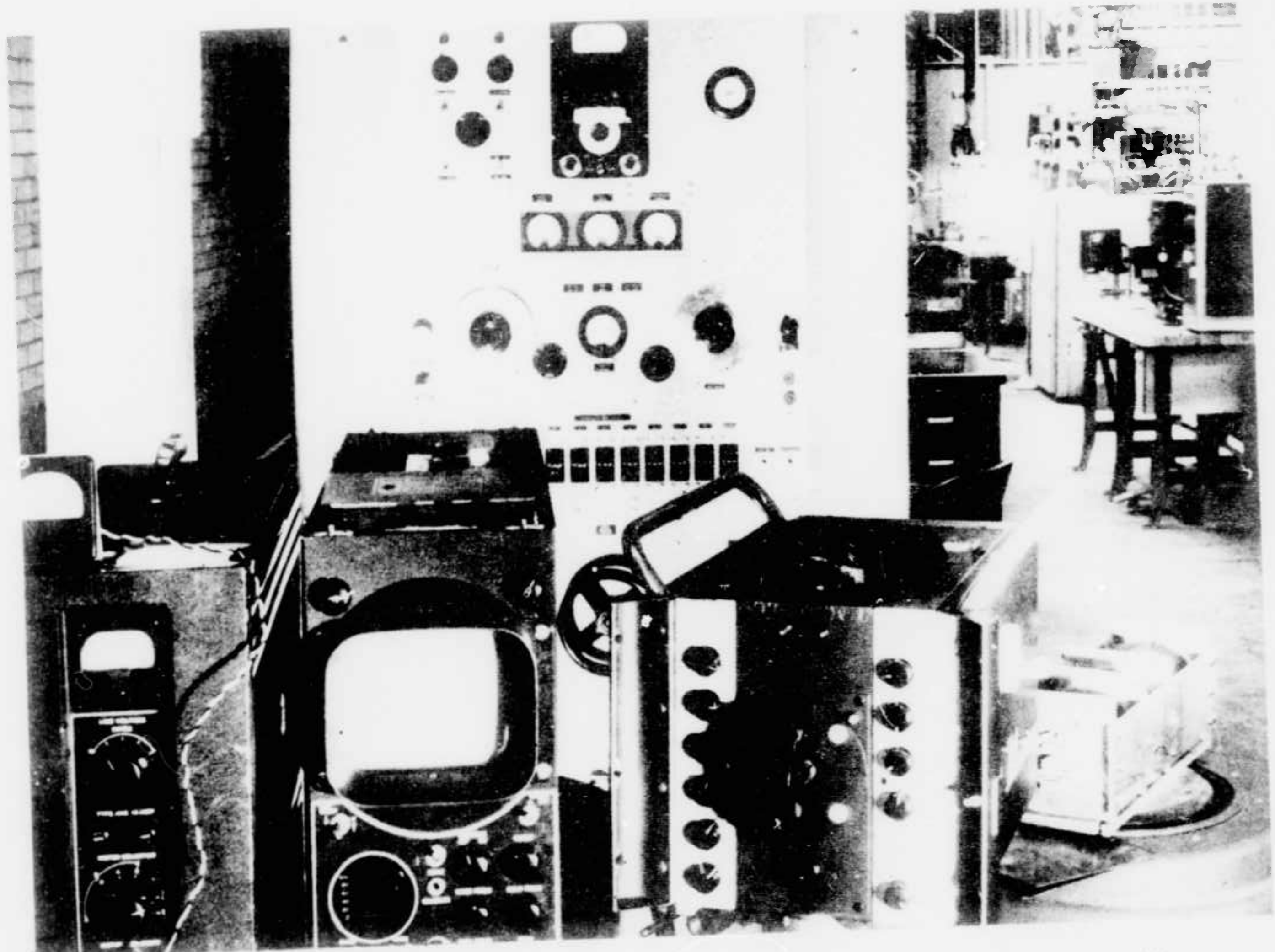

Figure 19. Equipment used with the electromagnetic vibration exciter. Front from left to right: power supply for camera and camera control, camera control, [illegible] camera. At center rear is the electronic control unit for the vibration exciter shown at lower right. The [illegible] is not shown.

A heavier vibration table capable of controlled amplitude vibration through the frequency of 5-2000 cycles/second was purchased under company sponsorship. Because of late delivery from the maker, the effective use of this table was not started until August 1, 1956. Contract No. AF33 (616) 2611 was extended from June 30, 1956 to October 28, 1956, primarily to obtain results with this new equipment from the image orthicon designs developed under the contract. Two jigs were designed for use on this table--one for transverse (X and Y axis) vibration, the other for Z axis, or longitudinal vibration. Care was taken in the design of these jigs to minimize cantilever suspensions and to prevent inherent resonant frequencies within the mounting in the desired 5-500 cycles test frequency.

It was found that the standard image orthicon yoke supplied by RCA for entertainment television use was not capable of withstanding 10G vibration. An intermittent blanking effect, which was initially laid to tube problems, was determined to be an intermittent contact on the focus coil. The alignment coil circuits opened frequently, due to the extreme fineness of the wire leads. When, late in the term of the contract, a ruggedized yoke was obtained for tube testing, many problems were then attributable to shoulder base socket contact sparking as they disappeared with the ruggedized yoke.

3. Image Formation During Microphonic Testing

In order to prevent relative motion of the tube and test pattern, a photographic film with the standard RTMA test pattern was taped directly to the faceplate of the image orthicon. As this film was stretched taut, it was unable to move significantly relative to the tube in any test.

4. Definition of Amount of Microphonics

Rather than attempting to quantitatively measure the amount of microphonics by calibrating an oscilloscope to measure the amplitude of the spurious signal, still photographs or motion pictures were taken of the image on the monitor while the tube was under vibration. Photographs, Figure17-19 , designate the amount of microphonics which are termed 17, no threshold of microphonics,18. significant amount of microphonics,19 unusable image. The reason for use of this type of test rather than the quantitative oscilloscope type was due to the difference in visual effect of the same amplitude of spurious signals.

E. Test Results

1. Patches

Patches are a microphonic signal which may appear on the monitor screen when an image orthicon is vibrated in the Z direction at accelerations as specified in environmental spec. Mil E5272A, Proc.1 in the range from

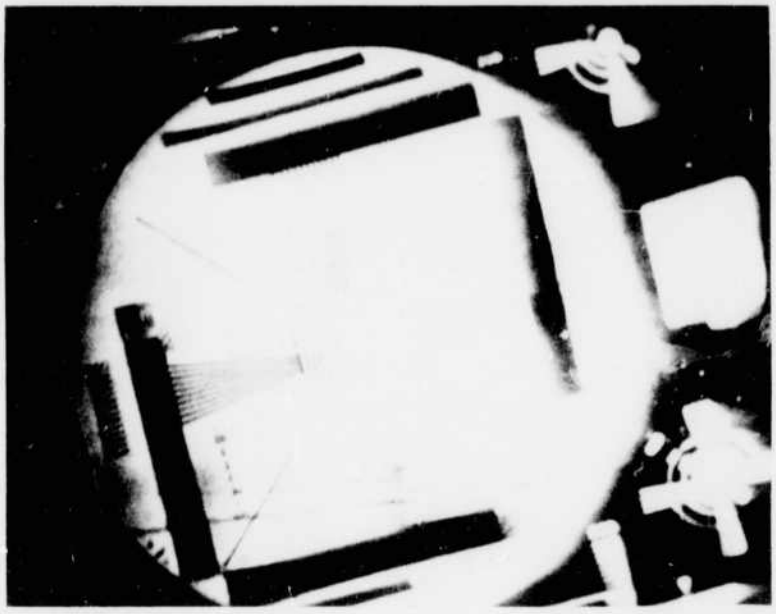

Figure 20 - Same tube as in fig. 18 and 19 with no vibration

Figure 21 - An illustration showing the line of demarcation between significant microphonics and microphonics which are not significant as defined for this report.

Figure 22 - Line of demarcation between significant microphonics and unusable microphonics as defined for this report.

60-100 cycles/second. They appear as small white areas with more or less well defined edges which cover several scanning lines. Because of the sequential nature of the scanning process in the monitor tube, this would seem to require than an electrical signal be generated within the camera tube or circuit at exactly 63 microsecond intervals to make up the parts of each "patch" which fall on successive scanning lines. Since this seemed too improbable, we concluded that the patches were "real" and that they were generated in some manner so that they could be scanned and imaged in the camera. Possible mechanisms would include the action of loose particles in the tube, perhaps very small glass chips, which might conceivable intercept the beam, land on the target or photocathode, or land on dynode #1 whose surface is scanned by the return beam. If the particles touched the target, they might influence the charge pattern.

To attempt to isolate the section of the tube where patches originate, we cut off the target, capped the lens, removed all voltages from the image section, even clipping the image section base pins to avoid contacts to the internal yoke wiring with no effect, except that some changes made the patches appear black instead of white. We tried disconnecting the dynode multipliers, one at a time, without result and tried overscanning the tube so that the return beam overscanned the first dynode and visualized the first pinwheel multiplier. Patches appeared over the whole field of view including the pinwheel. We tried disconnecting the deflection coils, a pair at a time, and the alignment coils, but blobs of light still appeared on the monitor indicating patches. When the scanning beam is cut off, there are no patches.

At the end of the contract, we had not discovered the mechanism of patches, but now lean toward the theory that they may be small particles intercepting the beam between the gun and the target. If so, they should be eliminated by further work spent on getting proper stem seal fillets around the leads, or by other steps toward even greater cleanliness.

It should be emphasized here that patches are not a serious problem. Our target specification Mil E 5272A, Procedure 1, requires that the tube be vibrated in simple harmonic motion with a double amplitude of .080" from 5 to 10 cycles/second and then with a constant acceleration of 0.4G from 10 to 15 cycles/second, then with a constant .036" double amplitude to 74 cycles/second, then at a constant 10G acceleration to 500 cycles/second. Patches occur primarily from 60-100 cycles/second at these specified amplitudes and accelerations. They are not visible at a constant 5G acceleration from 50-500 cycles/second, which exceeds the Mil E 5272A, Proc. 1 acceleration at 50 cycles. It can be assumed that patches will not be significant if the acceleration is reduced slightly to say 7 or 8 G in the range from 60-100 cycles/second. An image orthicon which will operate at 7 or 8G acceleration is useful in many Air Force and military applications.

Note that the extensive treatment of patches in the quarterly reports on this contract were based on vibration data taken at .080" double amplitude from 8 to 50 cps which is considerably more severe than Mil E 5272A, Proc. 1.

2. Imaging Quality vs. T-M Spacing

It has been shown earlier in this report, that the wider the target-to-mesh spacing, the better the microphonic performance. However, it is also shown that the image quality deteriorates as the spacing is increased. Two methods of increasing the spacing were tried. In one method, the target maintained its standard position and the mesh was moved inside the target support cup toward the photocathode to distances up to 100 mils. In the method termed "out spacing", the mesh maintains its normal position and the target is moved toward G5 up to 100 or 150 mils. It was found that the optimum compromise between microphonic and resolution performance was obtained by a 100 mil spacing where the mesh and target were each moved 50 mils from their original position. This was easily accomplished without using any exteraneous magnetic material. The standard mesh support ring was used in an inverted position. A 50 mil spacer of the type mentioned before, called a "radiused" spacer, moved the target out its required distance. The standard clamping arrangement is used.

3. Causes of Permanent Damage in Tubes

The basic design worked out under this contract appears sound. Failure through permanent damage to non-microphonic tubes of this final design can be laid to one problem—particles. These particles varied from small glass chips all the way up to components shaken loose during vibration. Tubes in the latter class have been opened and the cause in all cases was found to be poor weld quality. Proper operator training and use of precision welders has eliminated this problem. The small glass chips resulted from cracking of the image stem lead fillets during vibration. The remedy here is improved stem fabrication methods. The fillet around the leads must have the proper re-entrant angle to allow motion of the lead during vibration without glass chips.

4. Performance Data on Recent Tubes

During the first ten months of this phase of the contract, performance has been recorded by still photographs. However, these photographs do not present an accurate portrayal of tube performance, due to the visual effect of transients which cannot be shown in any still representation. During the last two months of the contract, 16mm movies have been taken of tubes at 5 and 10G acceleration in all three axes. While these movies do not give a complete presentation of the microphonic data on a tube, they show what performance can be expected from a given tube at a given level of acceleration at each frequency. Data was

taken from typical frames of this film to illustrate what is meant by significant microphonics. Graphs have been prepared of three recent non-microphonic tubes as compared to two standard Westinghouse factory shrinkage tubes. These graphs show the acceleration level which produces microphonics termed significant and the level which makes the tube unusable at 10 cycle intervals between 50 and 500 cycles. There is a wide variation in performance from tube to tube. This has been traced to variations in target and mesh tensions. It is shown by these graphs that the frequency between 150 and 300 cycles is the worst area for both the standard and non-microphonic tubes. An average chart of 3 non-microphonic tubes shown an acceleration level for significant microphonics of 4G as compared to 2G on the standard tube in this frequency range. From 350 cycles to 500 cycles, the non-microphonic tube showed the significant microphonics acceleration level approaching 10G while the standard tube runs through many resonant points where the significant level drops below 1G or within a few cycles rises to 5G's.

In order to set a single figure of merit on the tube design, it is necessary to make a very rough approximation. If the average value of accelerations for significant microphonics for all frequencies from 50-500 cycles were taken as this figure of merit the value for a standard Westinghouse 5820 image orthicon would lie between 2.5 and 2.75 G. For the non-microphonic Westinghouse WX3604, the same figure of merit would lie between 6 and 6.5 G. We believe that this difference would be more substantial if the comparison were made between the WX 3604 and 5820's made by our competitors. Current field reports from many television stations using both Westinghouse and competitors' tubes indicate that the standard commercial image orthicon made by Westinghouse definitely displays superior performance while subject to vibration.

F. Conclusion

A modification of the standard Westinghouse image orthicon has been created which shows significantly superior performance under vibration. The design parameters of this tube have been fairly well established. They are as follows: There are extra ceramics support rods and clamps wherever practical to make the electron gun and image structures rigid. There are bulb spacer springs which effectively strengthen the cantilever mounting of the image mount and gun assembly bulb spacer. The T-M spacing has been increased to 100 mils. By improved design the target tension has been increased 10 times and the mesh tension has been increased 25-50% over prior practice. The gun assembly is supported not only by the leads and the bulb spacers, but also by kovar buttons on the G3 electrode sealed to the glass wall. The dynode structures of the gun are securely mounted with ceramic spacers tightly fitted between them.

Use of precision welders by trained operators assured consistent strength welds. Careful stem fabrication eliminates feather edges which may result in loose glass particles in the tube during vibration. As redesigned, the WX3604 image orthicon is capable of satisfactory operation, under vibration at 4-5G acceleration from 50-500 cycles/second, at .036" double amplitude from 15-50 cycles/second, and at .080" double amplitude from 5-15 cycles/second.

While tube design of the WX3604 demonstrates significantly improved vibration performance, we do not consider it the ultimate which could be reached. However, further investigation of high strength high tension mesh structures will probably make further improvements possible. In our opinion, the present design approaches the limits of the improved performance possible using the standard gun and image structures. Other improvements will necessitate radical modifications of the internal assembly of the tube such as use of integral target mesh assemblies.

It should be noted that no testing of the tube was done with the faceplate down. The tube should still be operated in a position not exceeding 15° below the horizontal. It should also be noted that time did not permit operation of tubes for long periods at vibration frequencies which produced resonances in the tube.

In conclusion, the significant progress made under this contract toward the design of a non-microphonic image orthicon suitable for use in aircraft should be emphasized. In June 1955, this phase of the contract started as a feasibility study to determine whether the image orthicon could be made less microphonic. By June 1956, when adequate vibration testing equipment was received to make this test, our objective was to come as close as possible to meeting the conditions of Mil E 5272A, Proc. 1, a level of non-microphonic performance far in excess of the minimum required to make the image orthicon useful in aircraft flight.

Graph I

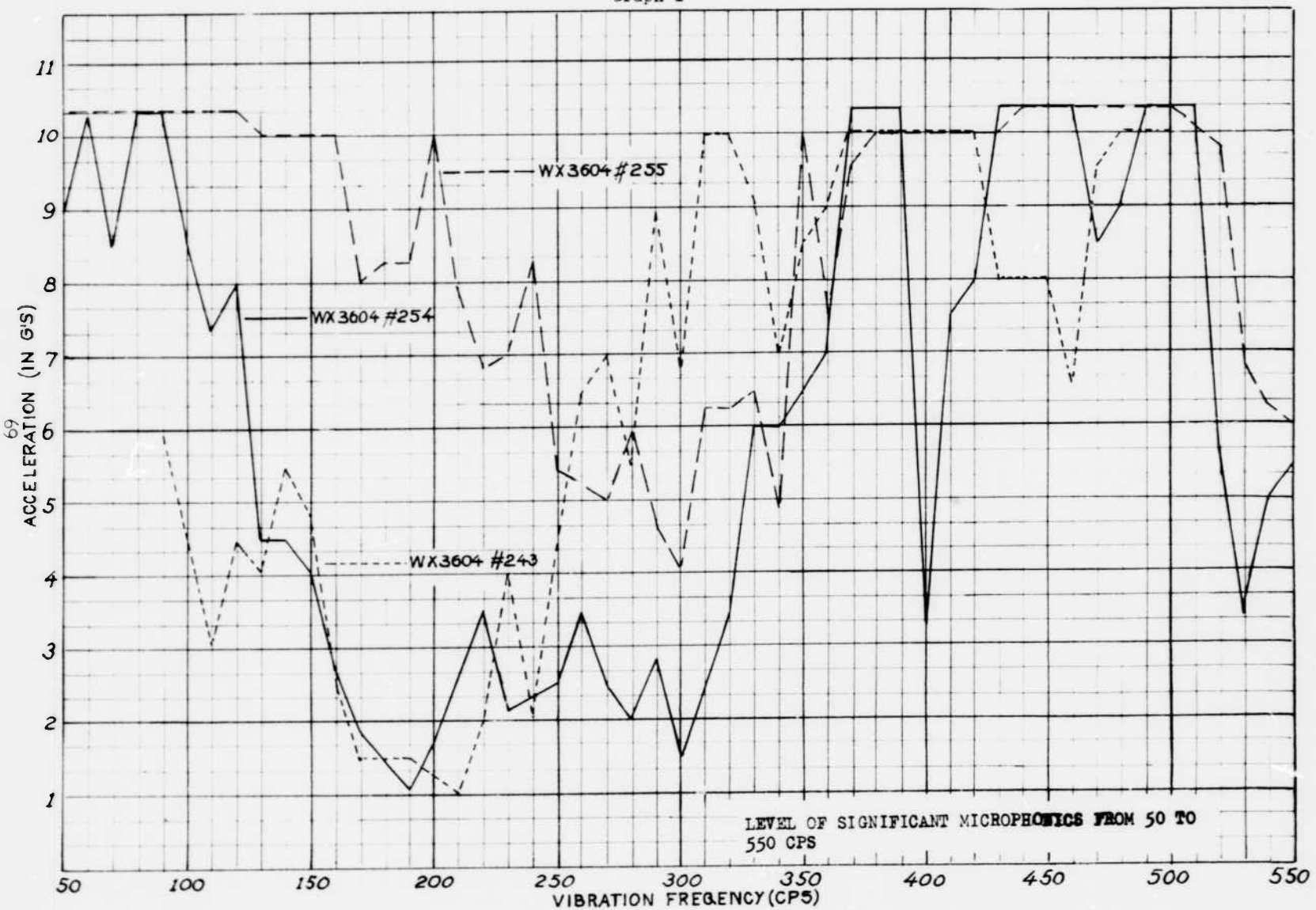
ACCELERATION (IN G'S)
VIBRATION FREQENCY (CPS)
WX3604 #255
WX3604 #254
WX3604 #243
LEVEL OF SIGNIFICANT MICROPHONICS FROM 50 TO 550 CPS
1
2
3
4
5
6
7
8
9
10
11
50
100
150
200
250
300
350
400
450
500
550

Graph II

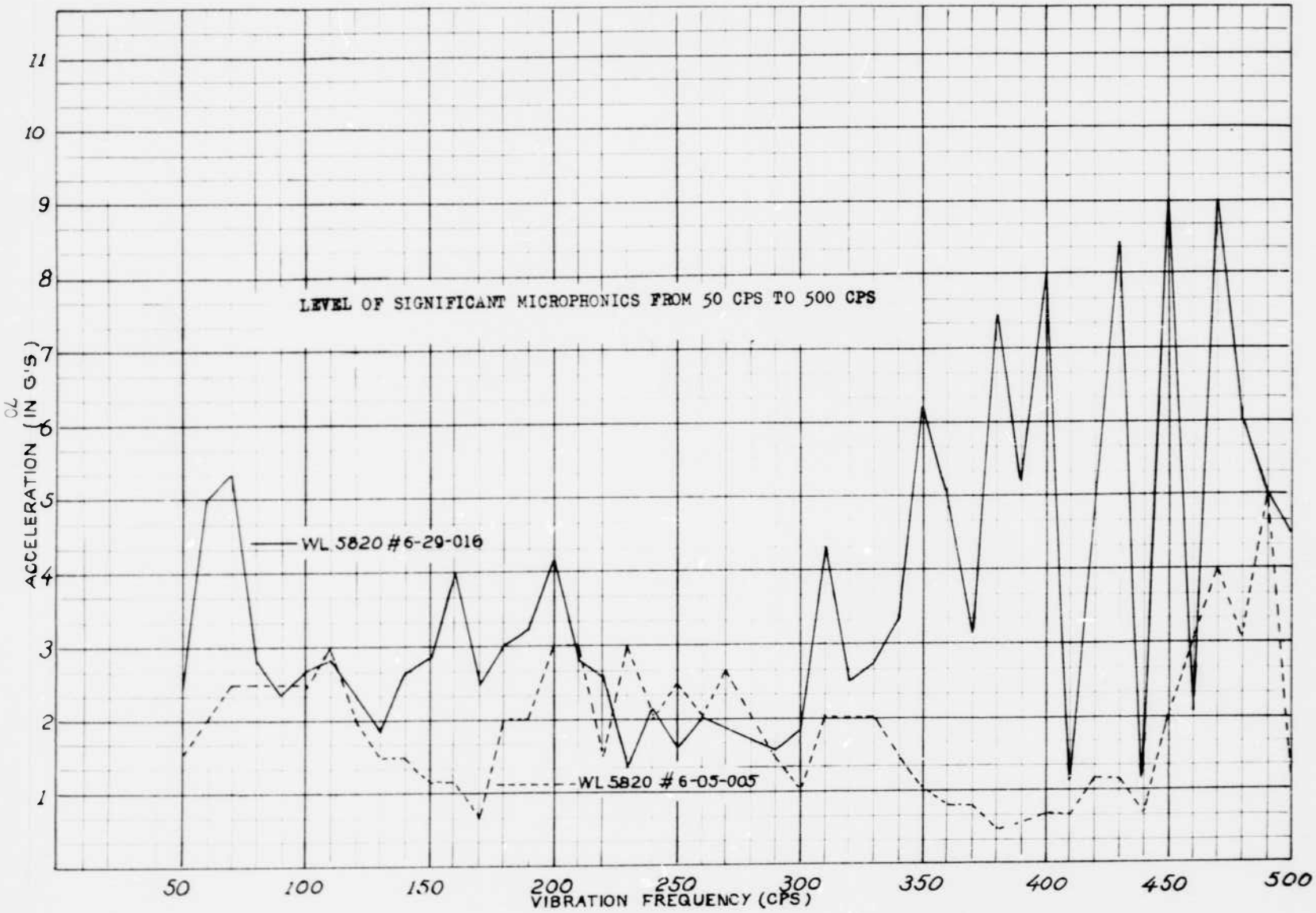
LEVEL OF SIGNIFICANT MICROPHONICS FROM 50 CPS TO 500 CPS
ACCELERATION (IN G'S)
VIBRATION FREQUENCY (CPS)
WL 5820 #6-29-016
WL 5820 #6-05-005
1
2
3
4
5
6
7
8
9
10
11
50
100
150
200
250
300
350
400
450
500

Graph III

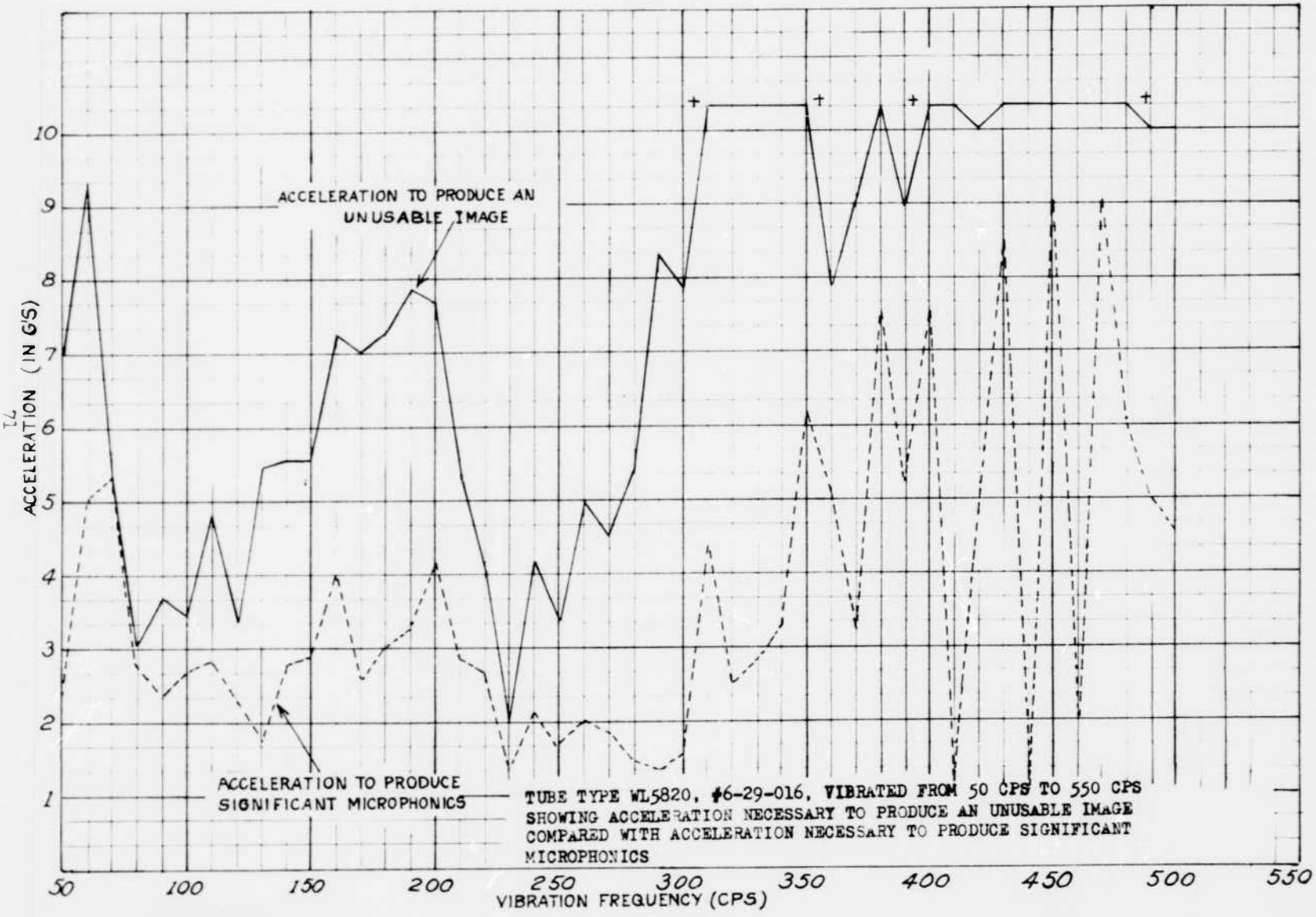

TUBE TYPE WL5820, #6-29-016, VIBRATED FROM 50 CPS TO 550 CPS SHOWING ACCELERATION NECESSARY TO PRODUCE AN UNUSABLE IMAGE COMPARED WITH ACCELERATION NECESSARY TO PRODUCE SIGNIFICANT MICROPHONICS

Graph IV

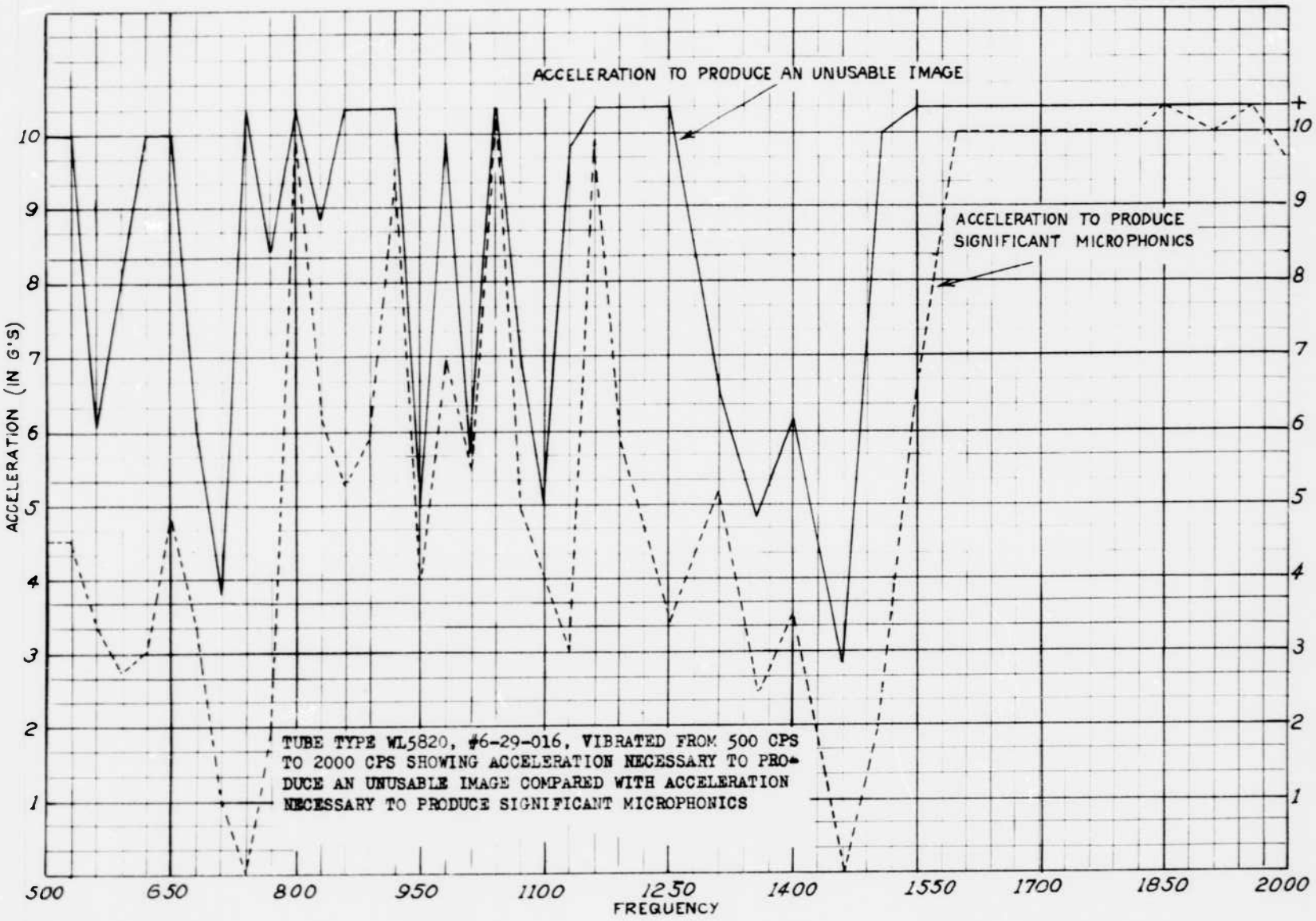

TUBE TYPE WL5820, #6-29-016, VIBRATED FROM 500 CPS TO 2000 CPS SHOWING ACCELERATION NECESSARY TO PRODUCE AN UNUSABLE IMAGE COMPARED WITH ACCELERATION NECESSARY TO PRODUCE SIGNIFICANT MICROPHONICS

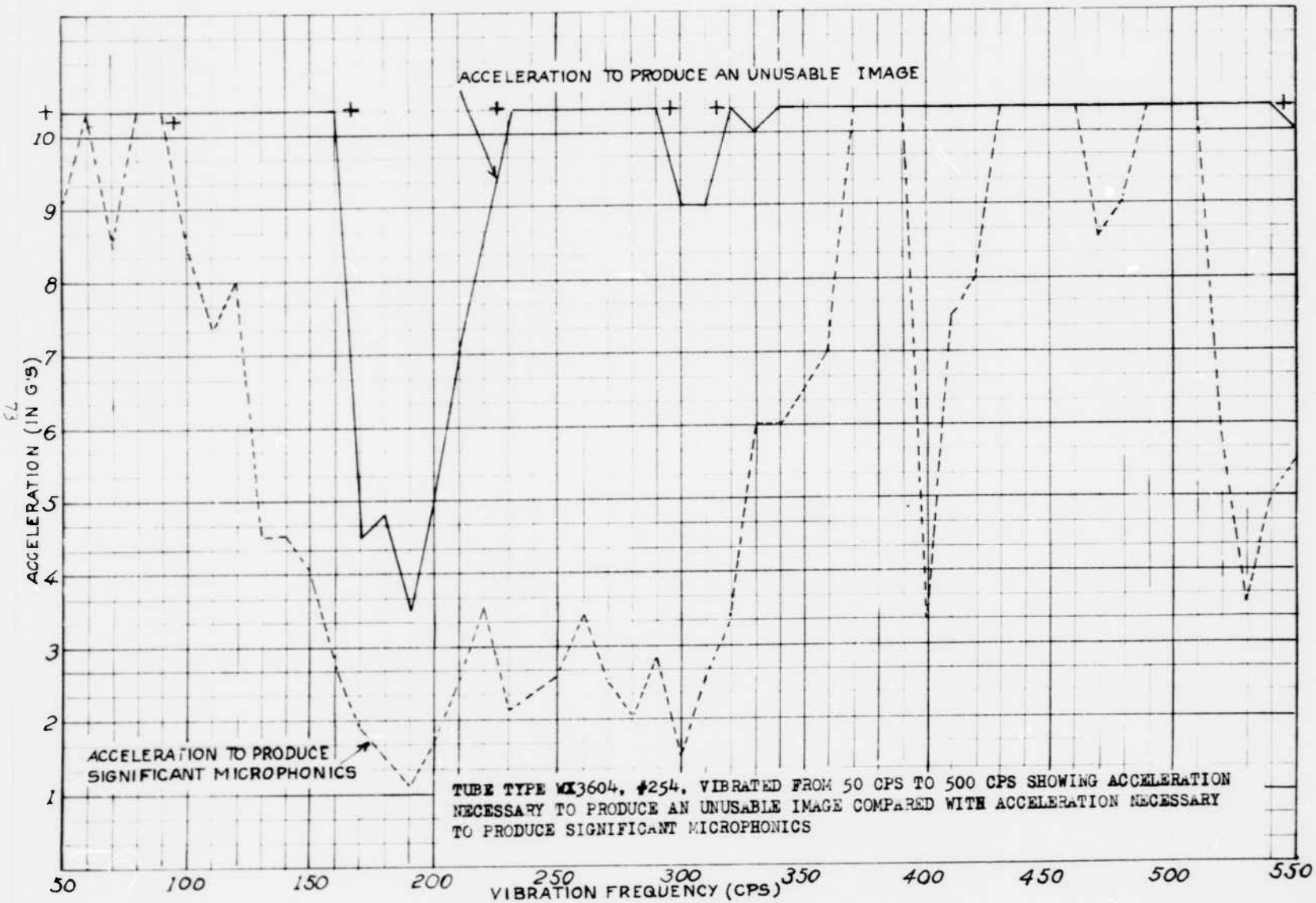

TUBE TYPE WX3604, #254, VIBRATED FROM 50 CPS TO 500 CPS SHOWING ACCELERATION NECESSARY TO PRODUCE AN UNUSABLE IMAGE COMPARED WITH ACCELERATION NECESSARY TO PRODUCE SIGNIFICANT MICROPHONICS

Graph VI

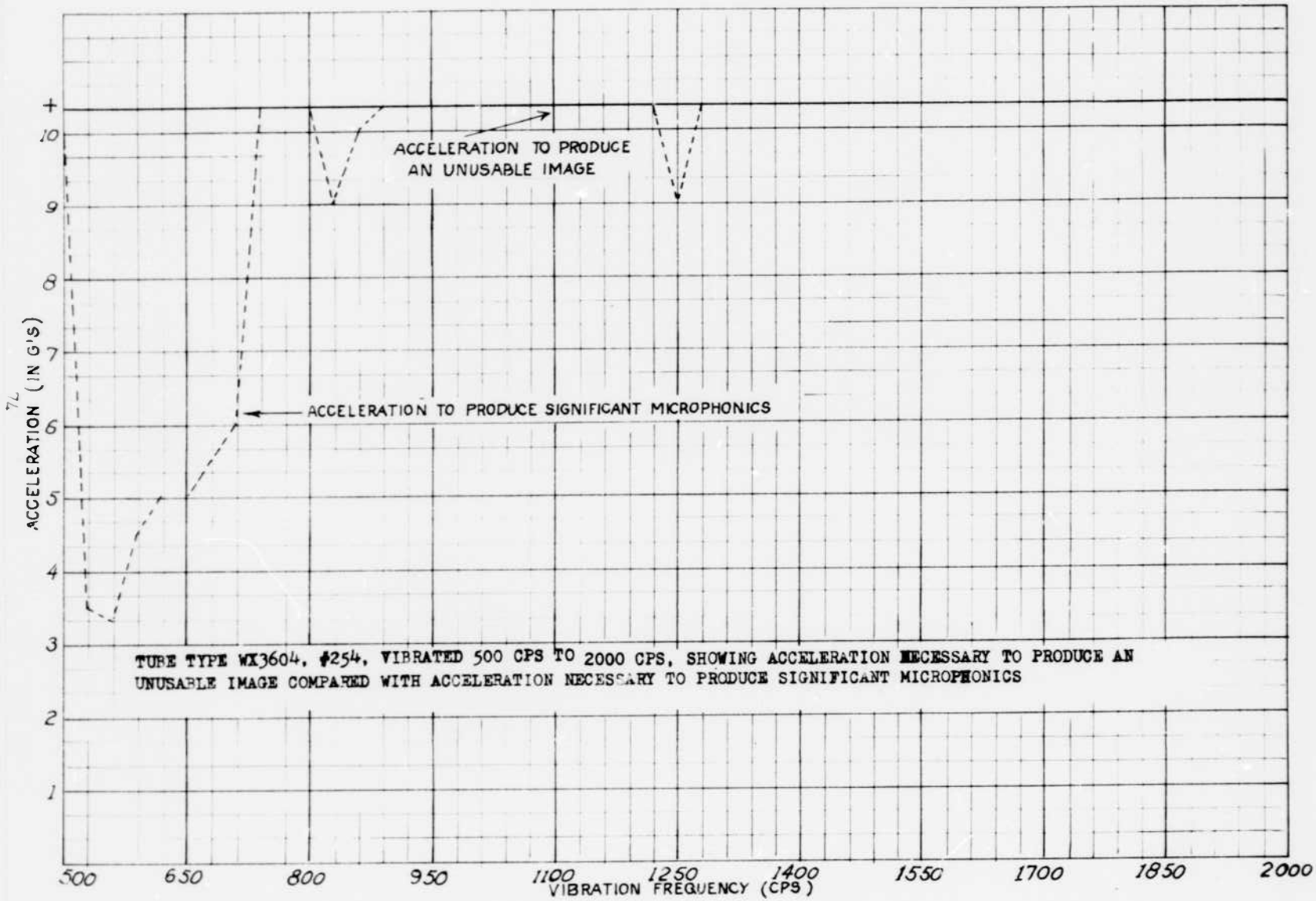

TUBE TYPE WX3604, #254, VIBRATED 500 CPS TO 2000 CPS, SHOWING ACCELERATION NECESSARY TO PRODUCE AN UNUSABLE IMAGE COMPARED WITH ACCELERATION NECESSARY TO PRODUCE SIGNIFICANT MICROPHONICS

Graph VII

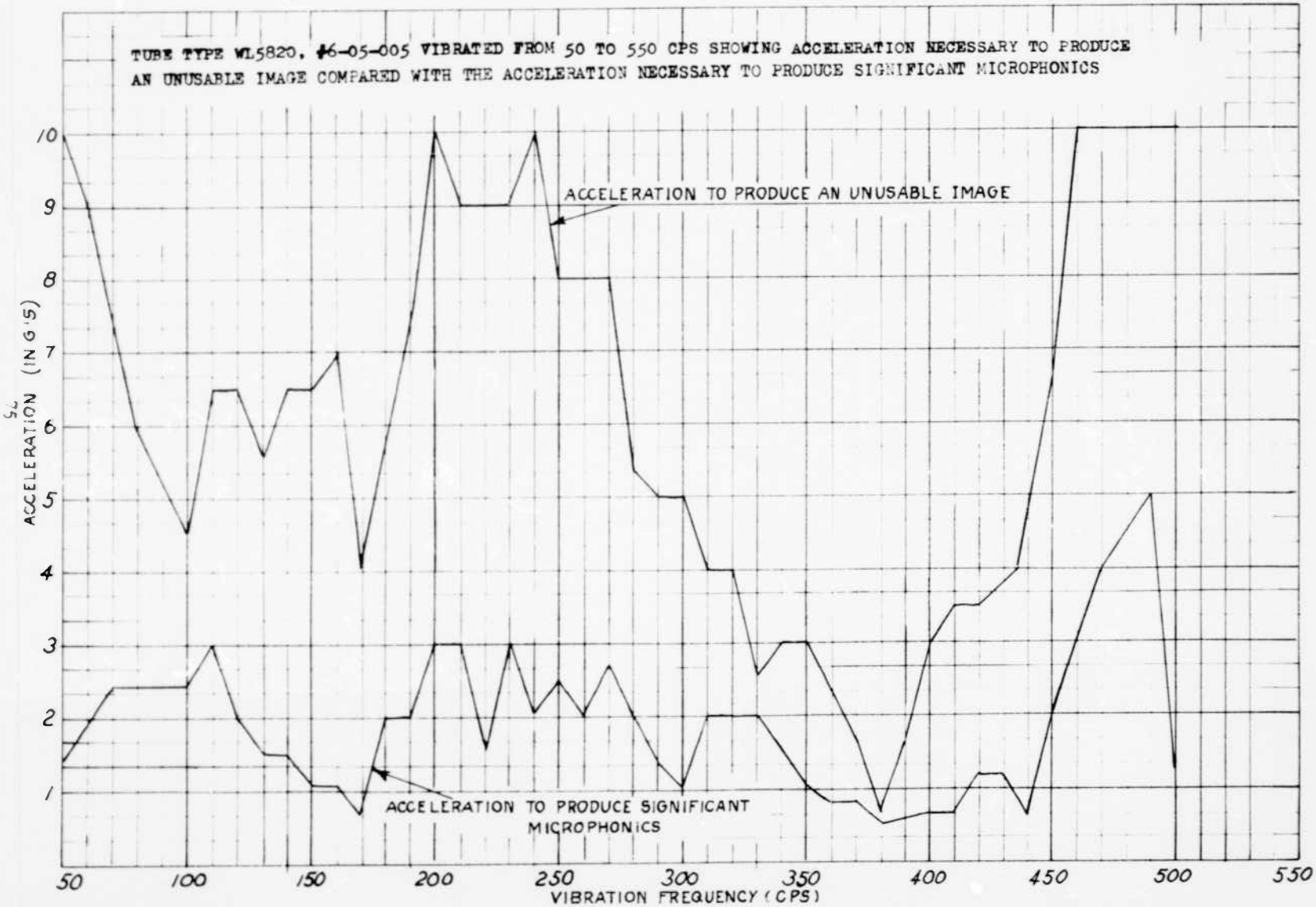
TUBE TYPE WL5820, #6-05-005 VIBRATED FROM 50 TO 550 CPS SHOWING ACCELERATION NECESSARY TO PRODUCE AN UNUSABLE IMAGE COMPARED WITH THE ACCELERATION NECESSARY TO PRODUCE SIGNIFICANT MICROPHONICS
ACCELERATION TO PRODUCE AN UNUSABLE IMAGE
ACCELERATION TO PRODUCE SIGNIFICANT MICROPHONICS
ACCELERATION (IN G'S)
VIBRATION FREQUENCY (CPS)
1
2
3
4
5
6
7
8
9
10
50
100
150
200
250
300
350
400
450
500
550

Graph .III

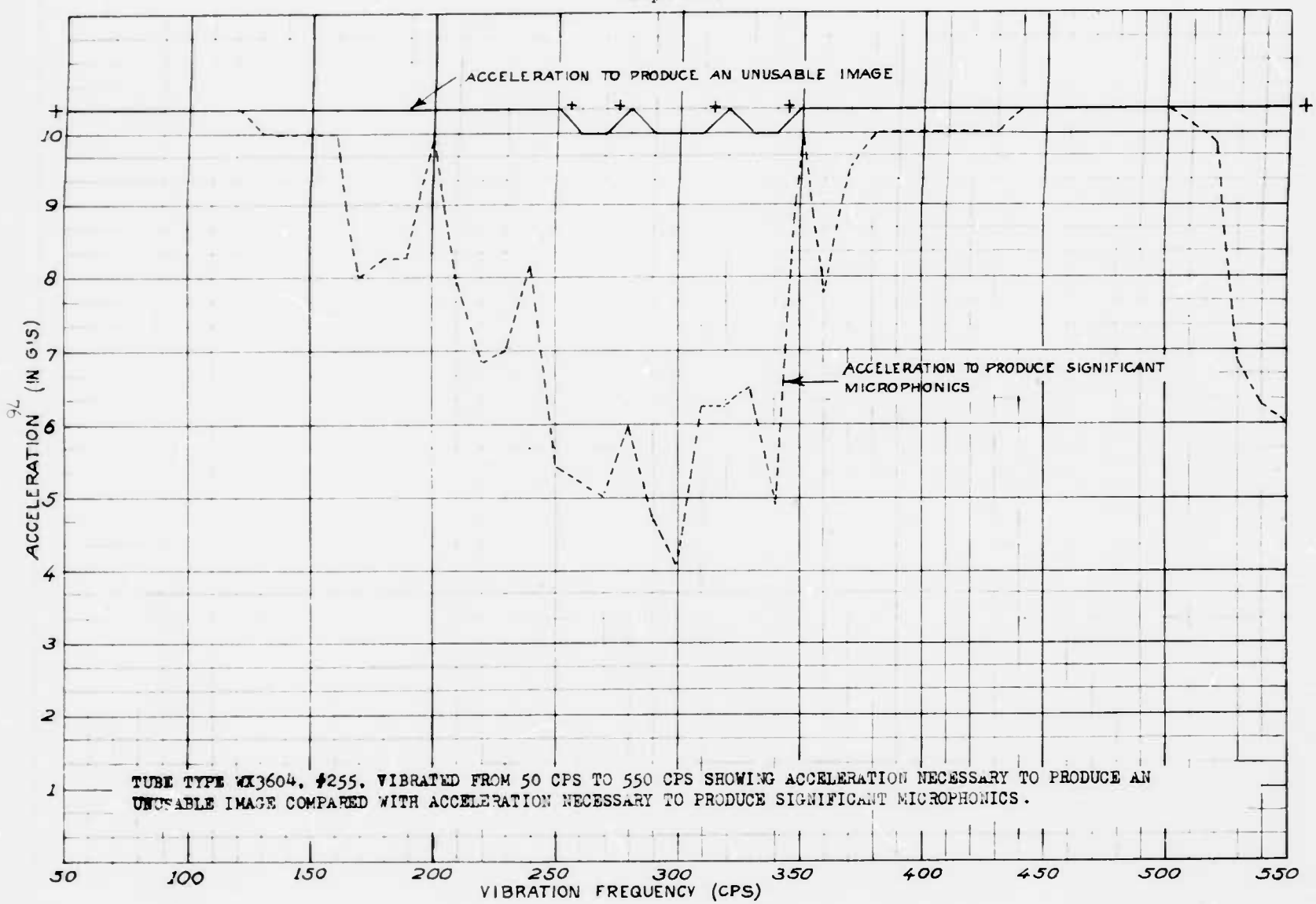

TUBE TYPE WX3604, #255, VIBRATED FROM 50 CPS TO 550 CPS SHOWING ACCELERATION NECESSARY TO PRODUCE AN UNUSABLE IMAGE COMPARED WITH ACCELERATION NECESSARY TO PRODUCE SIGNIFICANT MICROPHONICS.